University of Minnesota
St. Anthony Falls Hydraulic Laboratory

Project Report No. 185

THE DYNAMIC MIXED-FLOW MODEL FOR METROPOLITAN ST. LOUIS SEWER DISTRICT

by

Charles C. S. Song, Kim Sau Leung
and
James A. Cardle

Prepared for

Black and Veatch Consulting Engineers
St. Louis, Missouri

September 1979
Minneapolis, Minnesota

The Dynamic Mixed-Flow Model
For Metropolitan St. Louis Sewer District

Introduction

The existing facilities associated with wastewater overflows from the Bissell watershed include wastewater collection system elements in 23 sub-watersheds and flood protection facilities in 24 subsystems. Some collection system trunk sewers are over 125 years old. Portions of the existing trunk sewers have recently been rehabilitated as parts of pollution abatement and flood protection projects. Major flood protection works and pollution abatement facilities were completed in the last 10 years.

All collection system trunk sewers run in the general direction of west to east and have outlets at the Mississippi River. An intercepter sewer running parallel to the Mississippi River collects dry weather flow from most of the trunk sewers and carries it to the Bissell Point sewage treatment plant. Presently, sewage overflow problems exist during wet weather conditions, and also when the Mississippi River stage is higher than the crest of the diversion dam in the trunk sewer at the point of interception. When the river stage exceeds the high river stage, the intercepter gates are closed and sewage is discharged directly into the river.

Mandated by Federal law and under the sponsorship of the U.S. Environmental Protection Agency, the Metropolitan St. Louis Sewer District has contracted with Black and Veatch to study the possibility of eliminating the dry weather sewage overflow. As a part of this program, Black and Veatch has contracted with the St. Anthony Falls Hydraulic Laboratory to mathematically model the sewer system and to study the hydraulic characteristics which will be necessary for the evaluation of different design alternatives.

The model being used for the simulation of the St. Louis sewer system is the dynamic transient mixed-flow model recently developed at the St. Anthony Falls Hydraulic Laboratory. (This model is described in the Appendix.) The model is unique in that the complete kinematic and dynamic equations of motion for both open channel flow and pressurized flow phases are represented. Simultaneous occurrence of open channel condition and pressurized condition in any

segment of a sewer system can be accurately simulated. Various types of flow control devices, such as gates and pumps, are included in the model. Any predetermined inflow hydrographs representing dry weather and wet weather flows, as well as any alternative flow control algorithm, can be used as inputs. Velocity, discharge, and depth (or head) of the flow at any time and location can be computed and printed.

The model is an excellent tool for planning and design of a combined sewer system, serving the dual objectives of minimizing dry weather overflow and preventing flooding due to severe wet weather flow. Surges in open channel, wetwell, dropshafts, and water hammer in pressurized sections due to unsteady inflows and flow control maneuvering are important parameters limiting the safety and controllability of the system. Storage, overflow, pumping, and the rate of flow interception are parameters that define the system's effectiveness. Potential locations and the timing of bottlenecks and floodings need to be determined so that the necessary preventive measures can be taken. All of this information, which is needed for the design of the hardware and the software of a sewer and its control system, can be generated by this mathematical model.

Model Construction and Calibration

A total of four trunk sewer systems (Old Mill Creek, Harlem, Biddle, and Prairie) were modeled, but only the Old Mill Creek and the Harlem models were calibrated against the field data which were taken starting in November 1977.

First, in the spring of 1978, Black and Veatch conducted an extensive field survey on the portion of the sewer network in which the diameter equaled or exceeded 4 ft. Size, shape, length, and slope of the sewer were measured and recorded. All important structures, such as diversion structures, gates, pump stations, and relief structures, were also inspected and the conditions noted. Model systems' configurations were determined based on the field data as well as the original design drawings. The trunk sewer and a few major branches were usually included in a model.

Rainfall and flow depth data were taken by American Digital Systems, Inc. at strategic locations during the spring of 1978. Some of this data was used by Black and Veatch to calibrate the SWMM model. This calibrated SWMM model was then used to produce the design runoff hydrographs including the typical

hydrograph, the 30 year hydrograph, and the 100 year hydrograph at various input points to the dynamic flow model.

Synthetic runoff hydrographs corresponding to some storms which occurred during the spring of 1978 were also generated by the SWMM model. These runoff hydrographs were used as the input hydrographs to the dynamic model for calibration purposes. The model calibration was based on the comparison of the predicted flow depths with the measured flow depths at a number of locations in the system. Certain parameters (mainly Manning's 'n') were adjusted, if necessary, until close agreement between the model output and the field measurements was achieved. Figures 1 and 2 show the results of the calibration runs for the Harlem and Old Mill Creek models, respectively.

Old Mill Creek Sewer

The portion of the sewer system modeled is indicated in Fig. 3. The system's configuration, including station numbers, input points, relief structures, diversion structure, and the outlet work, is shown in Fig. 4. The trunk sewer is a horseshoe shaped tunnel about 3½ miles long. Five major branches to the trunk sewer were also included, making the total modeled length slightly over 7 miles. All of the simulations carried out for this system are listed in Table 1.

First, the model was run with a typical hydrograph having a recurrence interval of 1/12 year. It was found that the typical storm is so small that it causes no operating problem for the system. For the purpose of demonstrating how the proposed optimization alternative may work, the river was assumed at stage 26 (high river). The gate was initially closed and the pumps were not operating. A constant amount of flow, 81.2 cfs, was intercepted at the diversion structure. When the water level behind the flood gate rises above the river water, the gate is programmed to open at a rate of 1 ft per minute. When the water behind the gate drops below the river elevation, the gate is programmed to close at a rate of 1 ft per minute. This run is designated Run 1. The total inflow hydrograph, the discharge hydrograph, and the depth behind the gate are plotted in Fig. 5. Clearly, the typical storm is small enough for the system to function well. It is important to point out that the lag time between inflow and outflow is only about 15 minutes.

TABLE 1

Summary of Simulation Runs for

Old Mill Creek System

Run No.	Inflow Hydrograph	River Stage	Gate Operation	Pumping Operation
1	Typical	26	Controlled	No pumping
2	Typical	32	Closed	Flood control
3	30 year storm	-	Closed	Pumping when depth > 8 ft
4	30 year storm	26	Controlled	Pumping when depth > 8 ft
5	30 year storm	20	Controlled	No pumping
6	30 year storm	17.4	Controlled	No pumping
7	1/2 of 30 year	-	Closed	Pumping when depth > 8 ft
8	1/2 of 30 year	26	Controlled	Pumping when depth > 22 ft
9	1/3 of 30 year	32	Closed	Pumping when depth > 22 ft
10	1/4 of 30 year	32	Closed	Pumping when depth > 22 ft

The second run consists of the same typical storm occurring at a time when the river is at stage 32. The resulting hydrographs and the depth at the downstream end are plotted in Fig. 6. It is interesting to note that the gate never opened and that there was no outflow to the river. The constant interception rate of 81.2 cfs and the storage volume of the sewer were sufficient to prevent outflow in this case.

Since it appears that the flood protection work was designed to handle runoff from a 30 year storm, the Old Mill Creek model was run several times with the 30 year runoff hydrograph as the input. Various combinations of river stages, pumping conditions, and gate operating conditions were tried. The basic finding is that neither the sewer size nor the pumping capacity is sufficient to deal with this storm without the occurrence of serioud flooding. For example, Run 3 is conducted to test the adequacy of the pumping capacity. In this run, the river gates were assumed to be closed the entire time. Pumping was assumed to start when the depth at the downstream end reached 8 ft, and increased linearly with the depth until it reached the maximum pumping capacity of 2,850 cfs at a depth of 12 ft. Pumping for this run starts considerably earlier than the existing operating policy, which calls for the pump to start operating after the depth reaches 22 ft. The reason for starting the pump this early is to drain the system in order to provide maximum storage capacity for the peak flow. Figure 7 shows the total inflow hydrograph, the pumping rate, the depth in the sump, and the rate at which water is diverted to the New Mill Creek Relief Sewer at the seven relief structures. It clearly shows that the arrival of the flood peak is so abrupt that the depth at the downstream end increases very sharply at t = 325 minutes in spite of the pumping. Figure 8 shows some typical hydraulic grade lines in the trunk sewer at selected instances. Typically, for every run with the 30 year storm, the system first pressurized around station 60. This pressurized, or closed zone, rapidly spreads both upstream and downstream and eventually covers the entire trunk sewer. With such high head covering so large a portion of the system, flooding is inevitable.

Run 4 was made in order to test the effectiveness of flood gate operation in reducing the pressurization of the sewer. The river stage was set at 26 and the gate was allowed to open as soon as the water level became greater than the river level. The pump operating condition remained the same as that of Run 3. The resulting hydrographs are plotted in Fig. 9. It is interesting to note

that the gate opening occurred at such a late stage of the hydrograph that the total flow through the gate was negligibly small compared with the total runoff. Because the additional relief due to the gate opening is small, the entire system is again pressurized in much the same way as Run 3. Figure 10 is a graphic presentation showing the sequence of pressurization. It is typical for the 30 year storm to pressurize the two lower branches first and then spread upstream and downstream into the trunk line. This is an indication of inadequate tunnel capacity. The changes in water depth at the downstream end for Run 3 and Run 4 are plotted in Fig. 11 for comparison. The star on the graph indicates when the gate starts to open during Run 4. This graph shows a remarkable reduction in the water depth at the downstream end of the sewer due to gate opening. Unfortunately, this relief is very localized due to the sharpness of the inflow hydrograph and insufficient tunnel capacity.

Attempts were made to test the adequacy of the flood gates when the river stage was lower. In Run 5, the river stage was set at 20 and the gate was initially closed. The 30 year storm was applied to the system, and the gate was programmed to open at a speed of 1 ft/min when the water level exceeded the river stage. Figure 12 shows the computed outflow hydrograph and the depth at the downstream end. Figure 13 shows the cumulative volumes of inflow, outflow to the river, storage in the system, relief to New Mill Creek sewer, and the overflow to the street. This figure indicates that the system is still inadequate to handle the 30 year storm at river stage 20. The pressurization sequence of the sewer for Run 5 is depicted in Fig. 14. It again shows that pressurization first occurs at the Gratiot branch followed by gradual spreading to the entire trunk sewer. The river stage was further reduced to 17.4 and the computation repeated in Run 6. The resulting hydrographs and depth are plotted in Fig. 15. The improvement of performance due to lowered river stage is quite minor; the sewer still pressurized and overflow occurred. It appears that the system will not handle the 30 year storm even for very low river stages.

The inflow hydrograph due to the 30 year storm has a very steep shape and a peak flow rate of about 16,000 cfs. This is more than five times as large as the maximum flood pumping capacity of 2,850 cfs provided. Therein lies the major problem of the system. The next four simulations, Runs 7, 8, 9, and 10, were conducted in order to determine the maximum capacity of the system. First, the magnitude of the inflow hydrographs at every input point was reduced by a

factor of 0.5 without changing the time scale. Run 7 used this reduced hydrograph with the gate closed the entire time. The flood pumps were turned on when the depth in the sump exceeded 8 ft. The resulting hydrographs and depth in the sump are plotted in Fig. 16. As indicated by the fast rising depth in this figure (after t = 340 min.), the pumping capacity was inadequate even for this reduced storm. Nearly the entire trunk sewer was filled and some overflow was indicated. Because the existing structure does not allow for pumping until the depth exceeds 20 ft, the system cannot deal with the storm if the river gates remain closed.

The same reduced (½ x 30 year) storm was used for Run 8 under a somewhat different operating condition. The river stage was assumed to be at 26 and the gates were initially closed and programmed to open at a speed of 1 ft/min as soon as the water level at the outlet work exceeded the river stage. To take full advantage of the available pumping, the drain pump having the capacity of 342 cfs was turned on early to preserve the sewer storage capacity for the peak flow. The flood pumps were programmed to turn on when the level in the sump exceeded stage 32. The resulting hydrographs and the depth are plotted in Fig. 17. In this case, the opening of the gate prevents the water in the sump from rising much above the river stage, and a flood pump was turned on for only a brief period of time. Figure 18 shows the progress of pressurization during the course of Run 8. In this case, the Gratiot St. branch and the downstream end of the system began to pressurize at almost the same time. The pressurized zone spread to cover roughly the downstream half of the system near the peak flow, and then the system gradually opened up. Little or no overflow occurred for this run. That is how the optimized system would operate for a storm one half the size of the 30 year storm, provided the river was below stage 26.

As the river stage increases, the safe capacity of the system decreases. For example, at river stage 32, the pumping capacity is sufficient for storms equal to or less than 1/3 of the 30 year storm. Run 9 represents the case when the inflow hydrograph is equal to 1/3 of the 30 year storm runoff and the river is at stage 32. The flood gates were assumed to be closed. The drain pump was turned on at a rate of 342 cfs whenever the depth in the sump exceeded 8 ft in order to maintain as much storage volume as possible. The first flood pump was turned on as soon as the depth in the sump reached 22 ft. The full pumping capacity of 3,164 cfs would have been achieved at a depth of 25 ft. The resulting hydrographs and the depth are plotted in Fig. 19. It is

interesting to note that the depth never reached 25 ft and the full pumping capacity was not used. This result suggests the need to lower the intake elevation of the flood pumps. Because of the relatively high river stage and the depth at the downstream end, substantial portions of the sewer were pressurized. Hydraulic grade lines at two different times after pressurization are plotted in Fig. 20. The modest amount of head indicated in this figure should not cause serious flooding. The pressurization sequence for this case is shown in Fig. 21.

Finally, Run 10 was computed using an inflow rate equal to 1/4 of the 30 year storm runoff. All other conditions remained the same as those in Run 9. The resulting hydrographs are plotted in Fig. 22. Again the full flood pumping capacity was not realized. As indicated in Fig. 23, the downstream portion of the trunk sewer was pressurized. The pressure head in this case was somewhat less than that of Run 9.

Harlem Sewer

The portion of the Harlem Sewer system modeled is indicated in Fig. 24. The system configuration, including station numbers, input points, diversion structure, and the outlet work, is shown in Fig. 25. There are two major branches, 3.0 miles and 1.4 miles long, connected to a 1.6 mile long horseshoe shaped trunk sewer. A downstream portion of the sewer, roughly 0.5 mile long, is designed to operate at a pressurized condition during high flows.

A total of six runs, as listed in Table 2, was conducted using this model for the purpose of determining the system's capacity. Like the Old Mill Creek Sewer, this sewer is also sufficiently large to handle the typical storm without any problem. Figure 26 shows the inflow and outflow hydrographs and the depth at the downstream end due to a typical storm runoff when the river stage is less than 7.5 (Run 11). The system remains in the open channel flow condition during the entire storm period. The 30 year storm runoff at river stage 20 was used as the input for Run 12. The resulting hydrographs and the depth at the downstream end were plotted in Fig. 27. Two typical hydraulic grade lines are plotted for this run in Fig. 28. The lower line (t = 319.9 min) is for the system just before pressurization occurred. The upper line (t = 349.3 min) corresponds to the time of maximum outflow. The entire system is pressurized at this time, and a large portion of the system is subjected to

TABLE 2

Summary of Simulation Runs for

Harlem Sewer System

Run No.	Inflow Hydrograph	River Stage	Gate Operation	Pumping Operation
11	Typical	7.5	Controlled	Pumping when depth > 30.75 ft
12	30 year storm	20	Controlled	Pumping when depth > 30.75 ft
13	1/2 of 30 year	20	Controlled	Pumping when depth > 30.75 ft
14	1/3 of 30 year	20	Controlled	Pumping when depth > 30.75 ft
15	1/3 of 30 year	7.5	Controlled	Pumping when depth > 30.75 ft
16	1/4 of 30 year	20	Controlled	Pumping when depth > 30.75 ft

a pressure head substantially greater than 100 ft. Next, the inflow hydrographs were reduced to 1/2 of the 30 year storm runoff, and the model was run for a river stage of 20 (Run 13). The two selected hydraulic grade lines for this run are plotted in Fig. 30. The sewer is still completely pressurized during the peak flow period, but the maximum head was somewhat less than that of the previous run. For Run 14, the inflow hydrographs were further reduced to 1/3 of the 30 year storm while the river stage was kept at 20. Figure 31 shows the resulting hydrographs and Fig. 32 shows typical hydraulic grade lines. The maximum head has now been reduced to less than 100 ft. Run 15 uses the same inflow hydrographs used for Run 14, but the river stage was reduced to 7.5. The results are shown in Figs. 33 and 34. Only about half of the system is pressurized to a head of about 50 ft at the time of maximum flow. Finally, the input hydrographs were reduced to 1/4 of the 30 year storm runoff and tested at river stage 20. The results are shown in Figs. 35 and 36. In this case, only the 1.6 mile long downstream trunk sewer was pressurized with the maximum head of 30 ft.

The capacity of the Harlem Sewer to handle storm runoff is highly dependent on the river stage. At river stage 7.5 it may safely take 1/3 or even up to 1/2 of the 30 year storm. When the river stage is at 20, the system is marginal for a 1/3 x 30 year storm. The 30 year storm is too severe for the Harlem Sewer system regardless of the river stage.

Conclusions

The Old Mill Creek, Harlem, Biddle, and Prairie trunk sewer systems were mathematically modeled. The Old Mill Creek and Harlem sewer models were calibrated and evaluated. The results of this evaluation are listed below.

1. Neither the Old Mill Creek sewer nor the Harlem sewer has sufficient capacity to carry the 30 year storm runoff without the risk of serious flooding.
2. The carrying capacity of both sewers is affected by the river stage - the higher the river stage, the smaller the capacity.
3. The safe capacity of the Old Mill Creek sewer is limited by the pumping capacity when the river is at stage 32. Under this condition, the system can carry the runoff equivalent to 1/3 of the 30 year storm runoff.

4. When the river stage is reduced to 26, the safe carrying capacity increases to 1/2 of the 30 year storm runoff. This increased capacity is attributed to the opening of the flood gates when the water level in the sewer exceeds that of the river.

5. A further reduction in the river stage would probably increase the capacity to slightly more than 1/2 of the 30 year storm runoff.

6. The Old Mill Creek sewer can take a storm equivalent to 1/4 of the 30 year storm for the highest river stage possible.

7. The storage capacity of the Old Mill Creek sewer is large enough to completely store the typical storm runoff for future treatment.

8. The capacity of the Harlem sewer, in terms of storm sizes, is somewhat less than that of the Old Mill Creek sewer. To carry the storm equivalent to 1/2 of the 30 year storm, the river stage has to be equal to or less than 7.5.

9. When the river stage is increased to 20, the capacity is reduced to 1/3 of the 30 year storm.

10. The lag time between the peak inflow and the peak outflow for the Old Mill Creek sewer is about 15 minutes. For the Harlem sewer this lag time is only about 10 minutes. The implication is that the automatic control should be primarily based on the downstream condition. Information on rainfall and a real time predictive model is needed to gain greater lead time.

11. The use of automatic controls to prevent overflow and, at the same time to minimize the flood risk, can be achieved for storms less than 1/2 of the 30 year storm. Major systems modifications are needed if greater storms are to be dealt with.

12. The great majority of storm runoffs can be stored and treated by the Old Mill Creek system.

13. Because the lag time between the peak inflow and the peak outflow is short, automatic control is essential to achieving the objective of preventing dry weather outflow without increasing the flood risk.

Recommendations

1. Because it is feasible to prevent dry weather overflow without increasing the flood risk by means of automatic control, and because every sewer system has different characteristics, it is necessary to model more trunk sewers. It is recommended that a total of 12 trunk sewers, including the four already modeled, be modeled for the purpose of automatic control design.

2. Because large sewers, such as the Old Mill Creek sewer, are large enough to store the majority of storm runoffs, it is recommended that the objective of storage for treatment of storm runoff be given high priority.

3. It appears that many of the trunk sewers are inadequate to prevent flooding for storms equal to or greater than the 30 year storm without major facility improvements. Therefore, the flood control objective should also be given the same priority. At least the systems' capacities should be re-evaluated in as much as they will limit the ability to prevent dry weather overflows.

LIST OF ILLUSTRATIONS

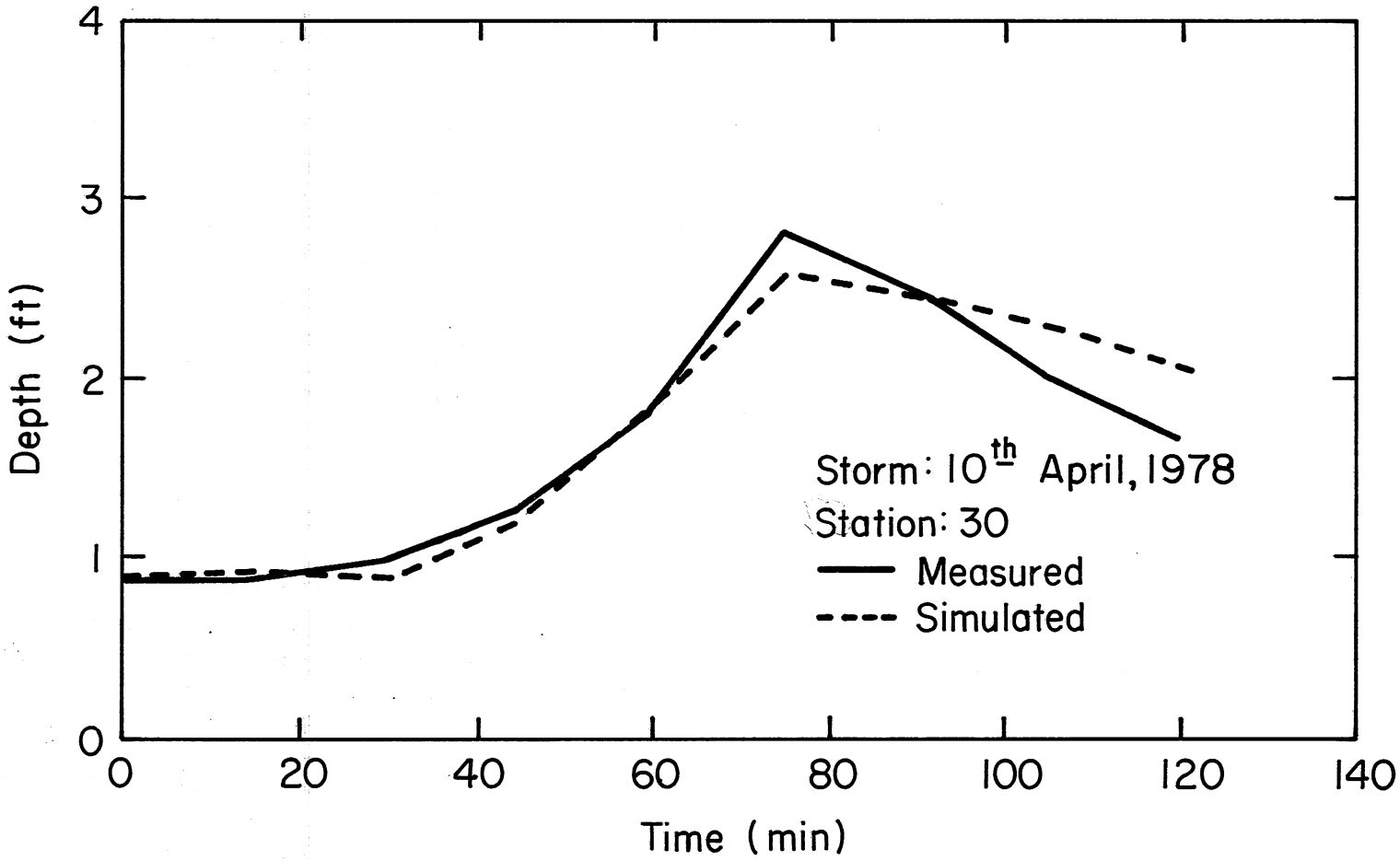

Fig. 1 - Comparison of Simulated Depth with Measured Depth, Harlem Sewer.

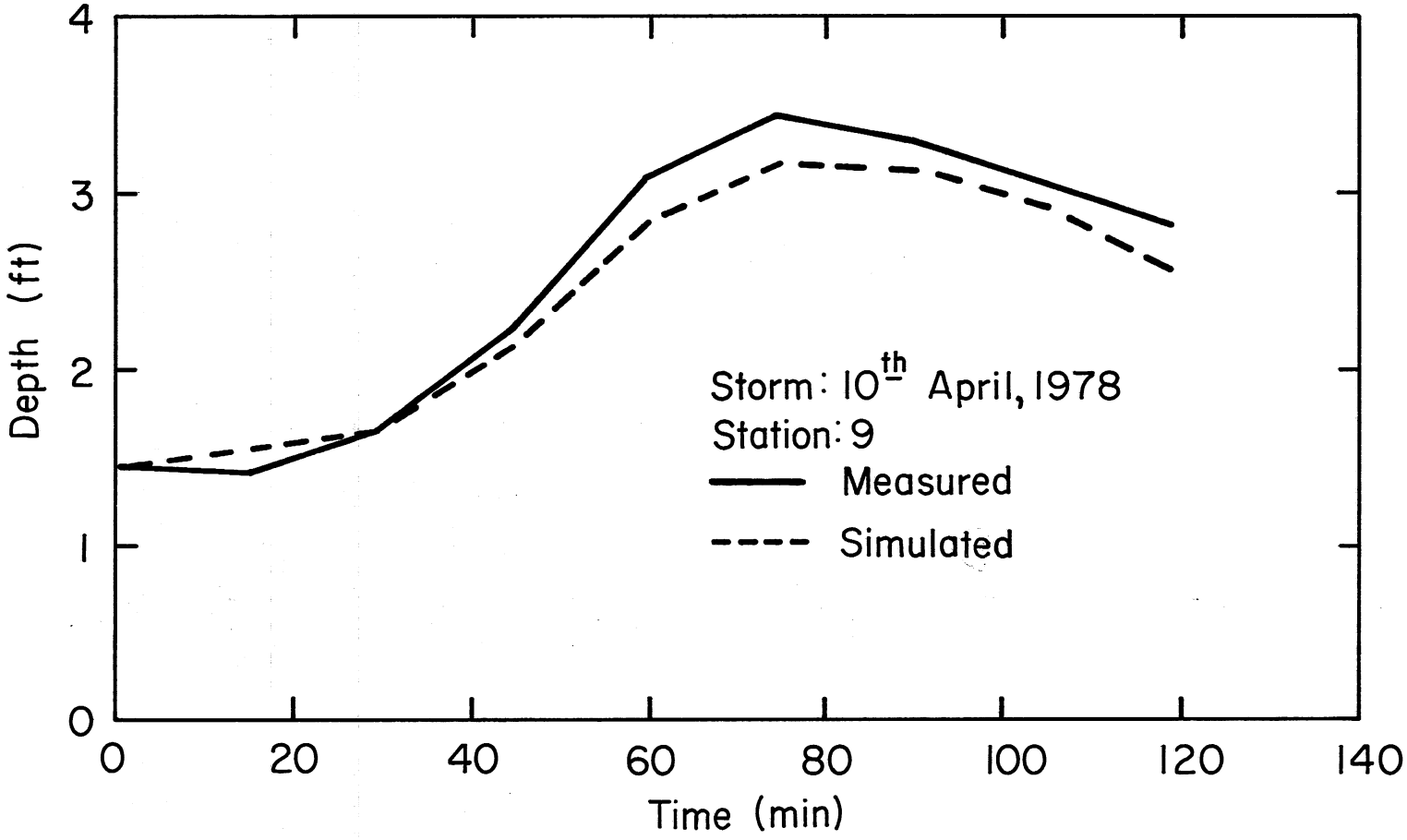

Fig. 2 - Comparison of Simulated Depth with Measured Depth, Old Mill Creek Sewer.

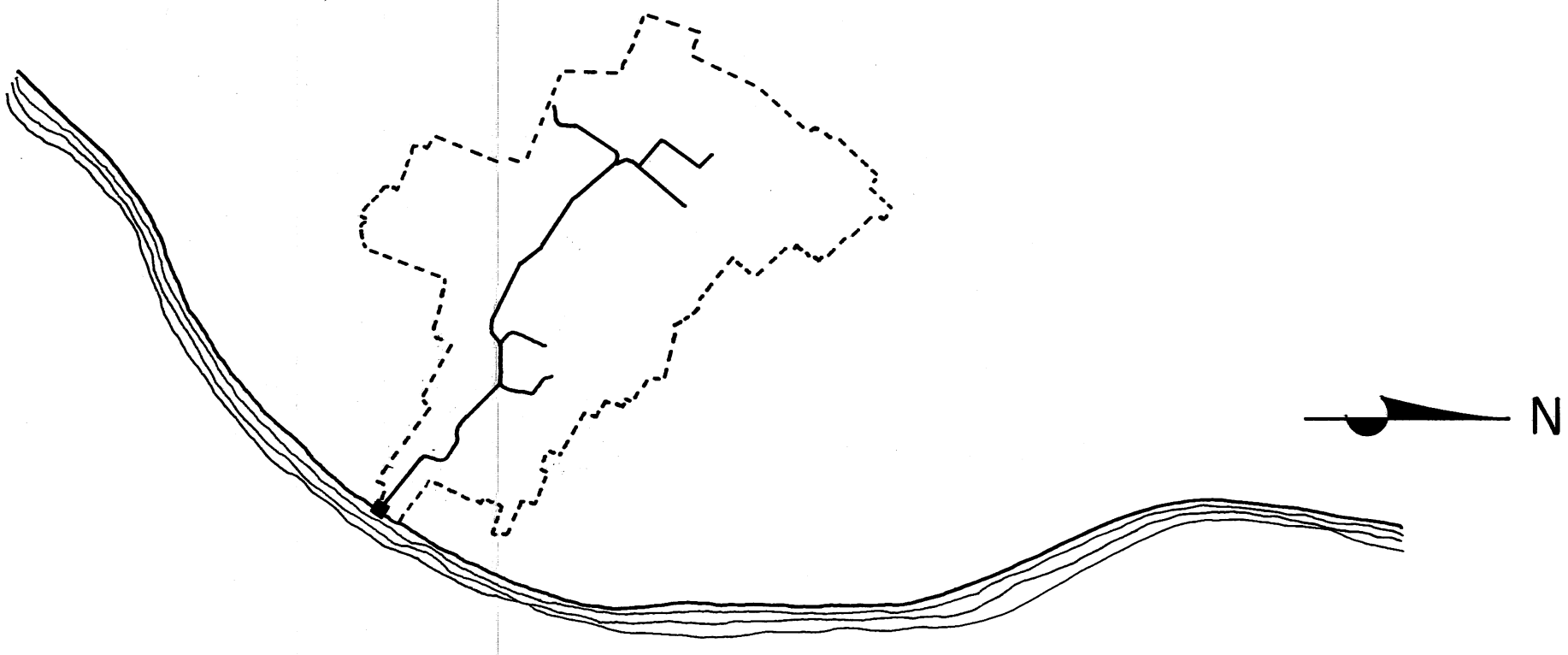

Fig. 3 - Maps Indicating Old Mill Creek System Modelled.

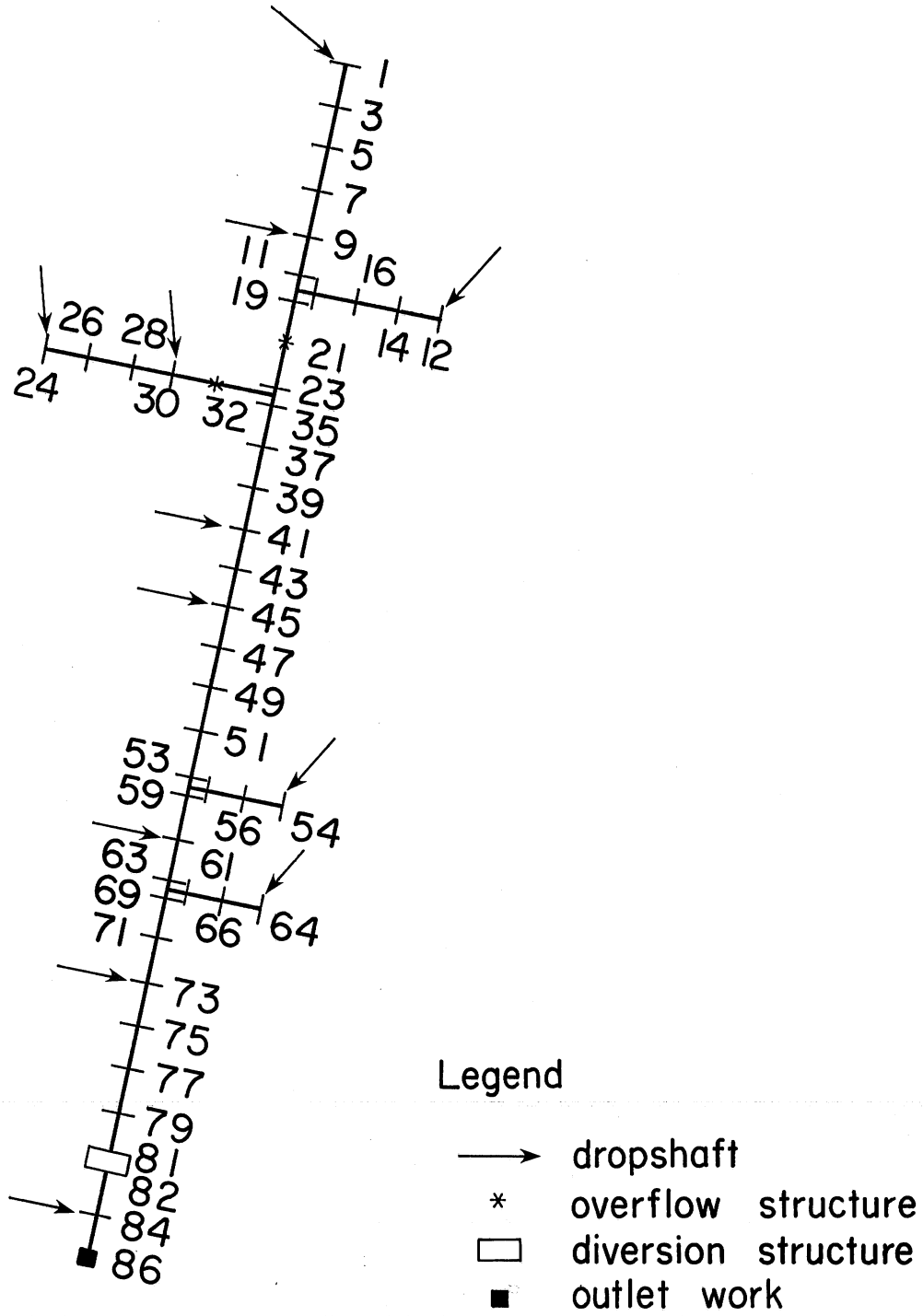

Fig. 4 - Old Mill Creek System Configuration.

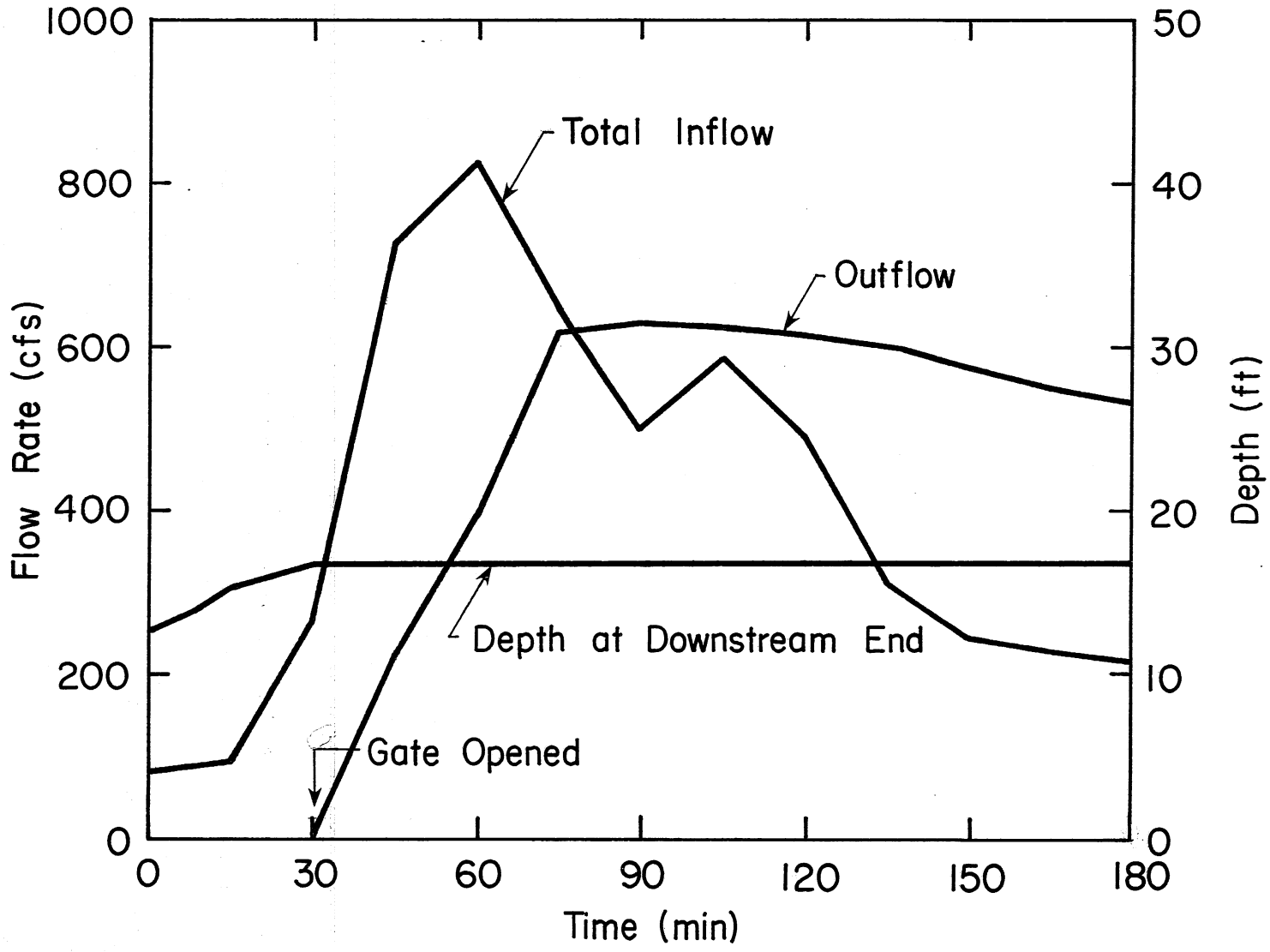

Fig. 5 - Hydrographs and Depth at Downstream End, Run 1, Old Mill Creek, Typical Storm, River Stage 26.

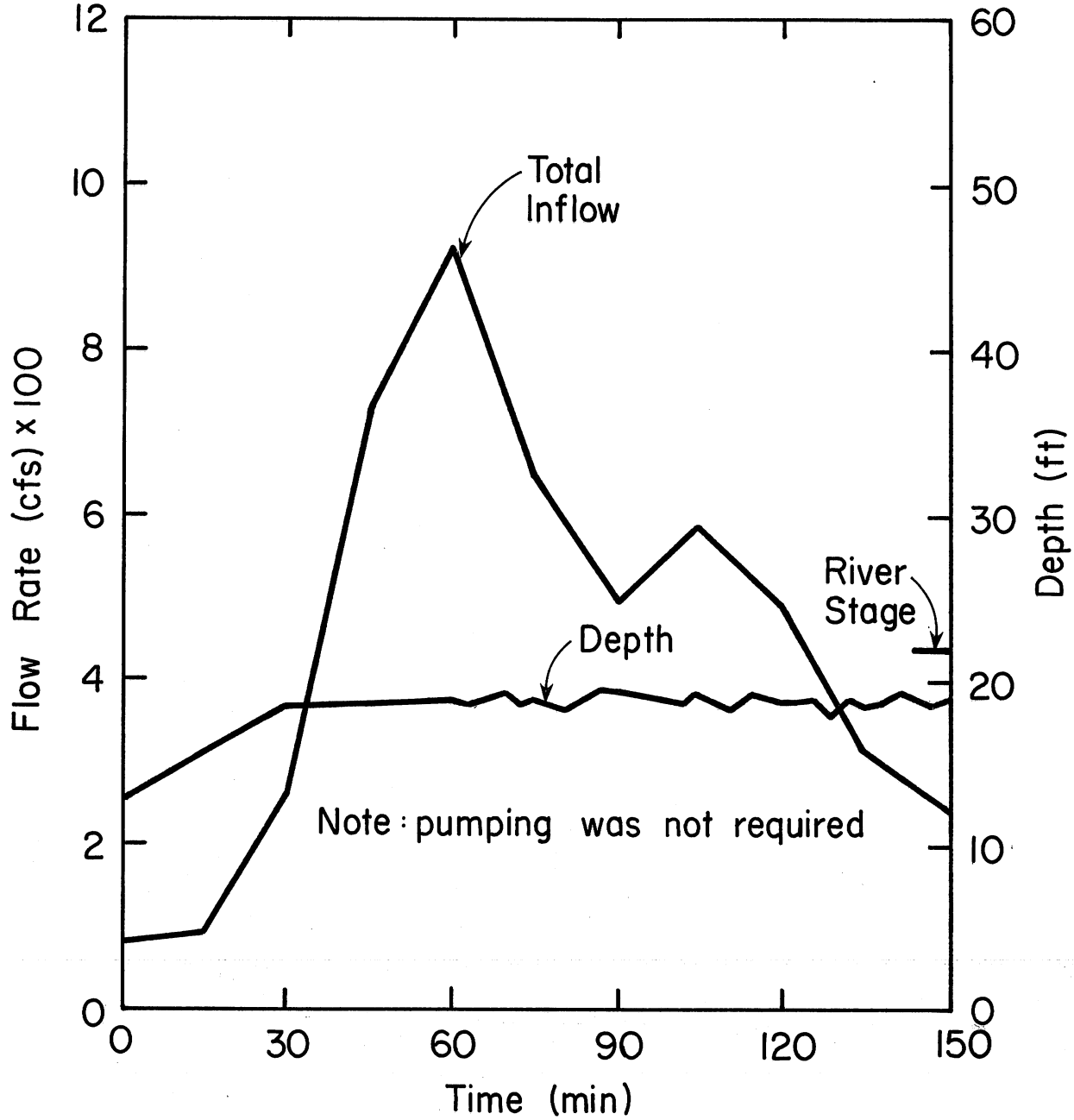

Fig. 6 - Inflow Hydrograph and Depth at Downstream End, Run 2, Old Mill Creek, Typical Storm, River Stage 32.

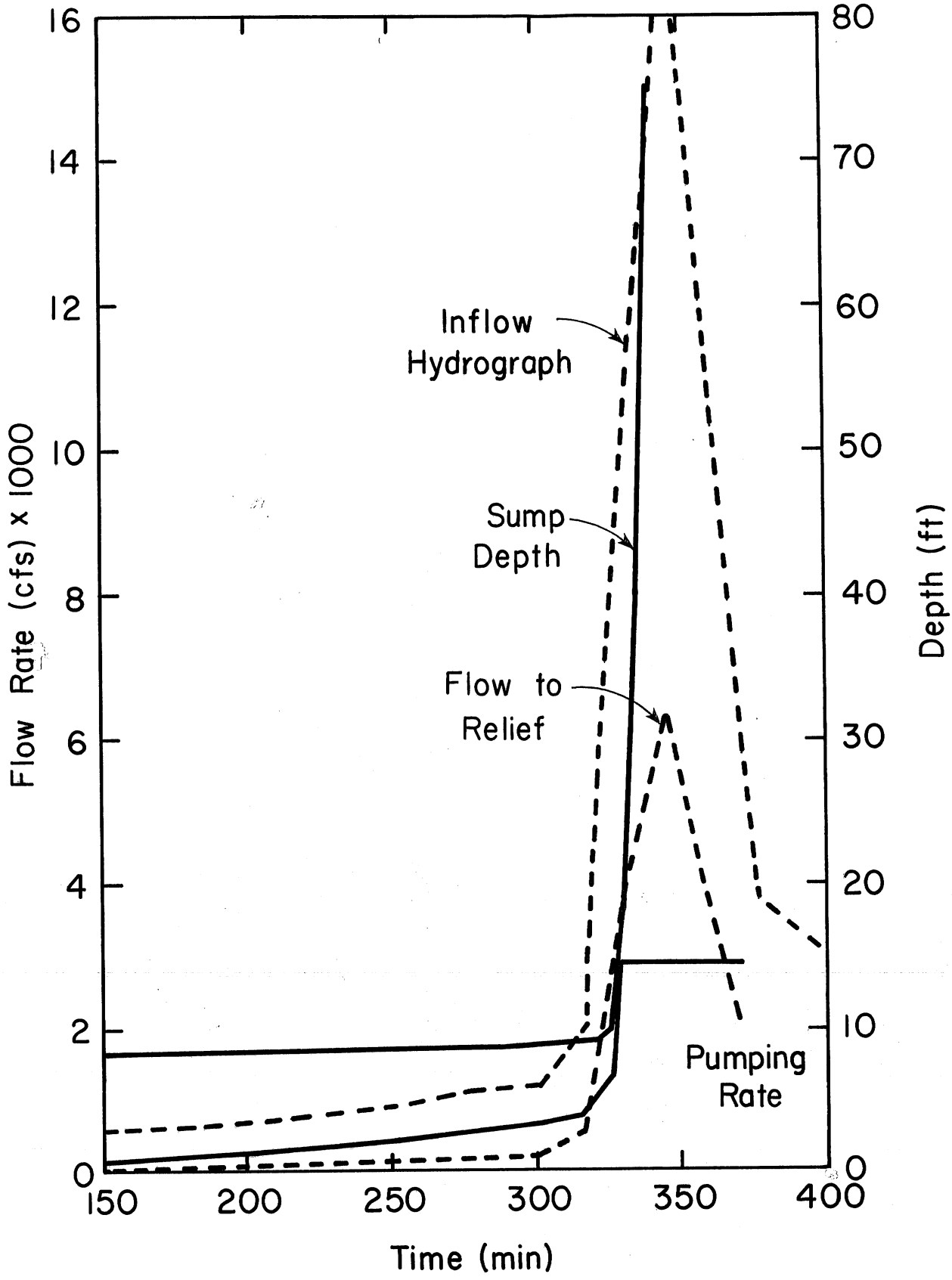

Fig. 7 - Hydrographs and Depth at Downstream End, Run 3, Old Mill Creek, 30 Year Storm Gate Closed.

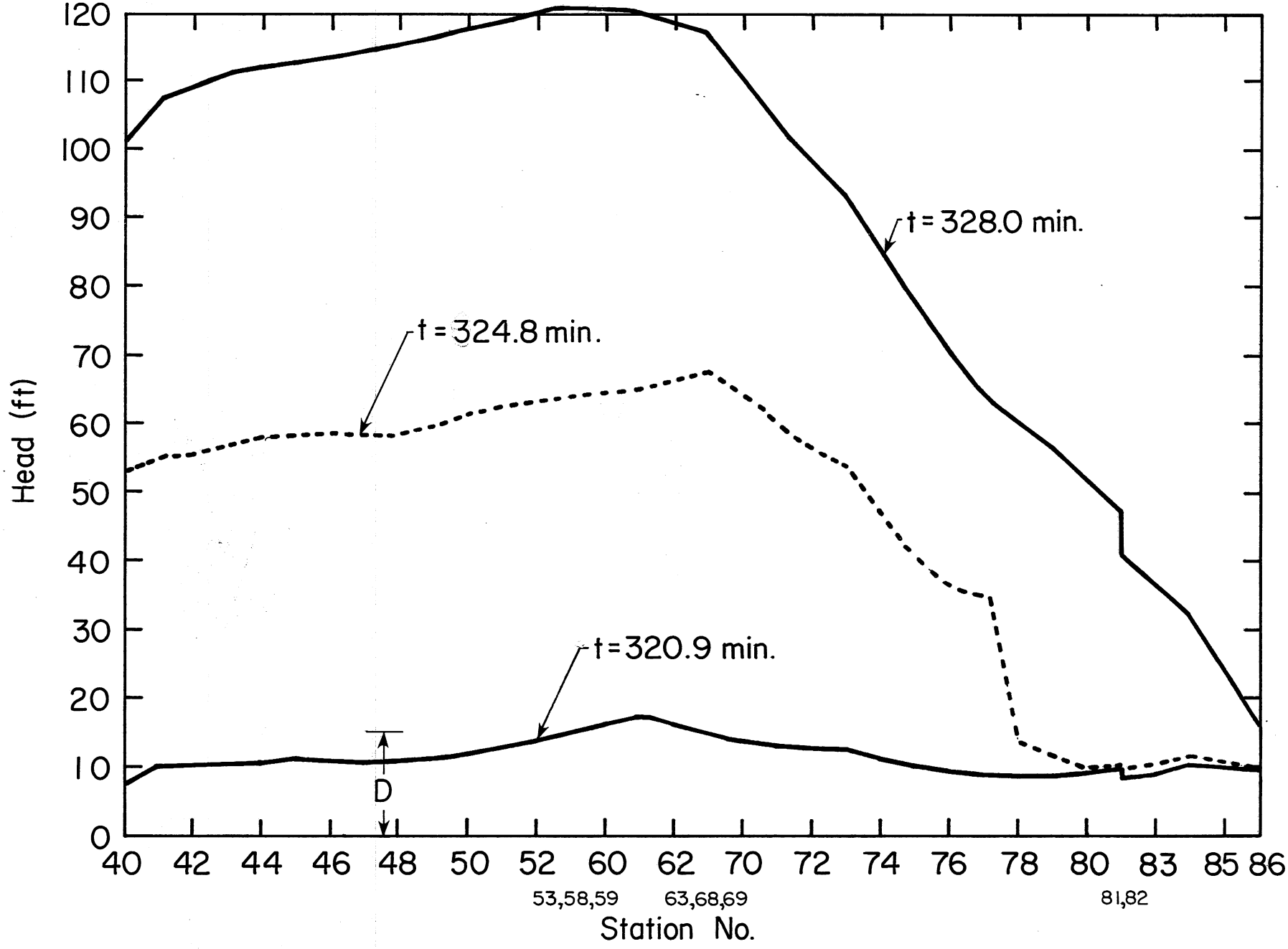

Fig. 8 - Hydraulic Grade Line, Run 3.

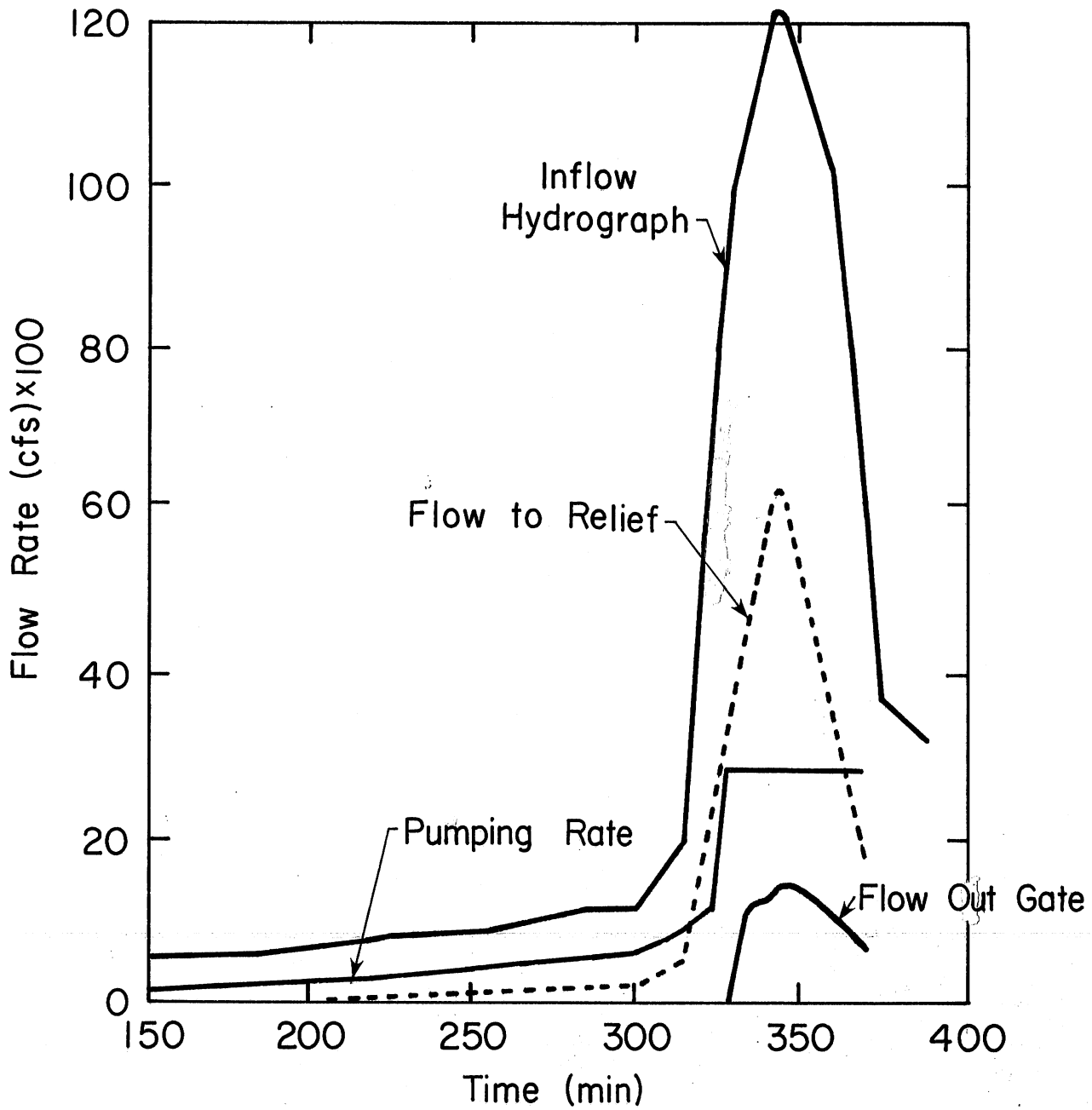

Fig. 9 - Hydrographs for Run 4, Old Mill Creek, 30 Year Storm.

Fig. 10 - Pressurization Sequence for Run 4.

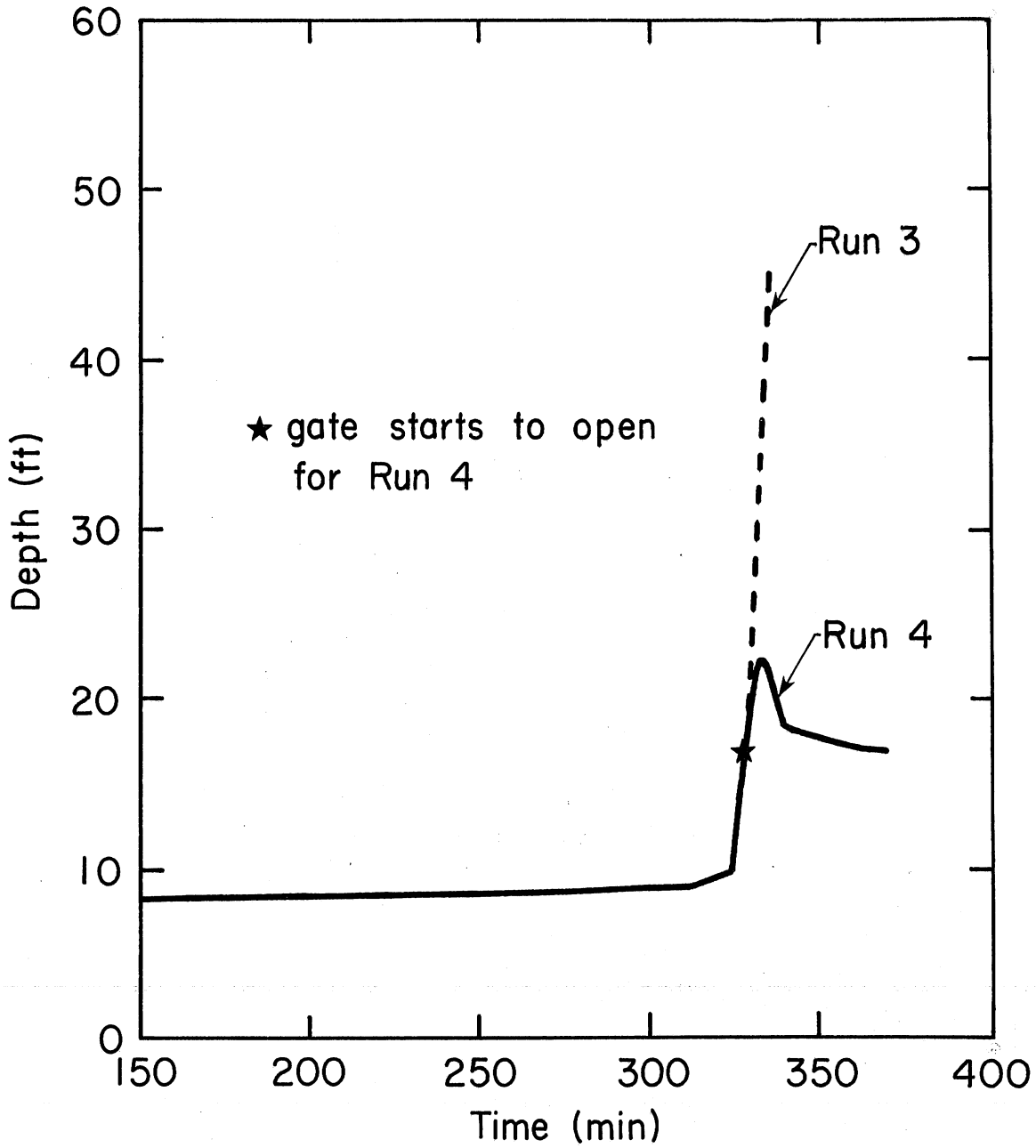

Fig. 11 - Comparison of Depth at Downstream End, Run 3 and Run 4.

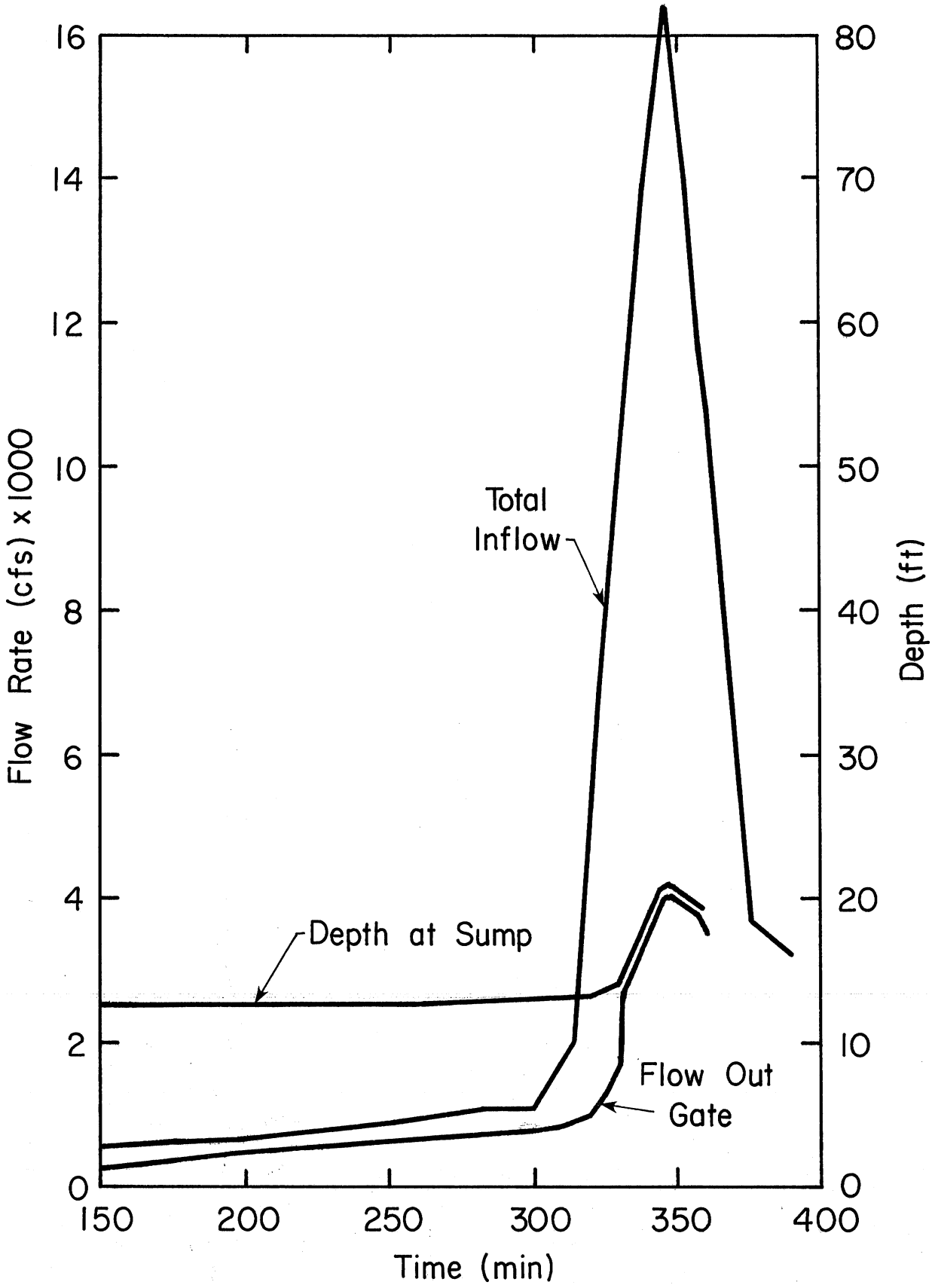

Fig. 12 - Hydrographs and Depth at Downstream End, Run 5, Old Mill Creek, 30 Year Storm, River Stage 20, Gate Controlled.

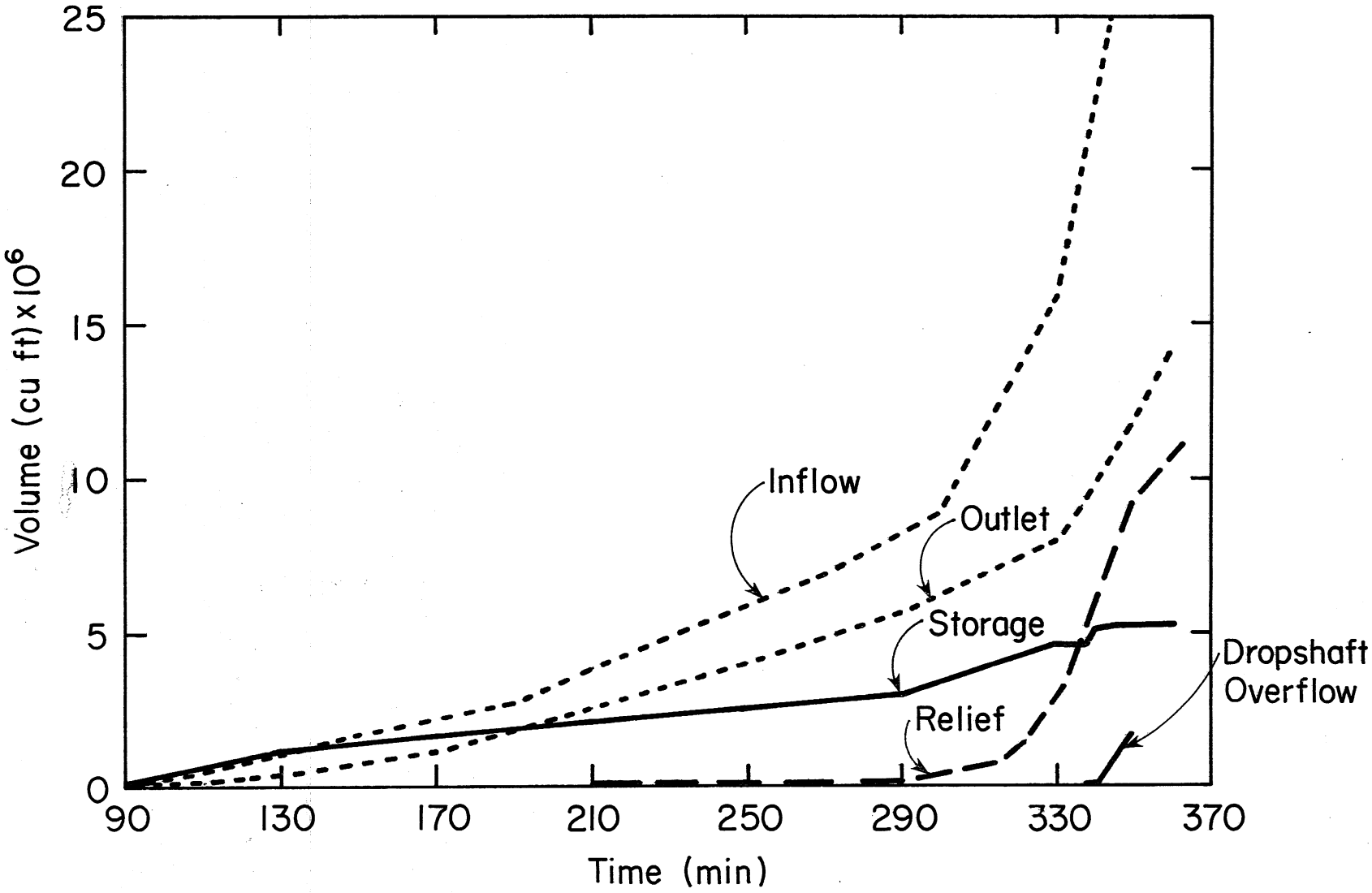

Fig. 13 - Cumulative Volume of Flows for Run 5.

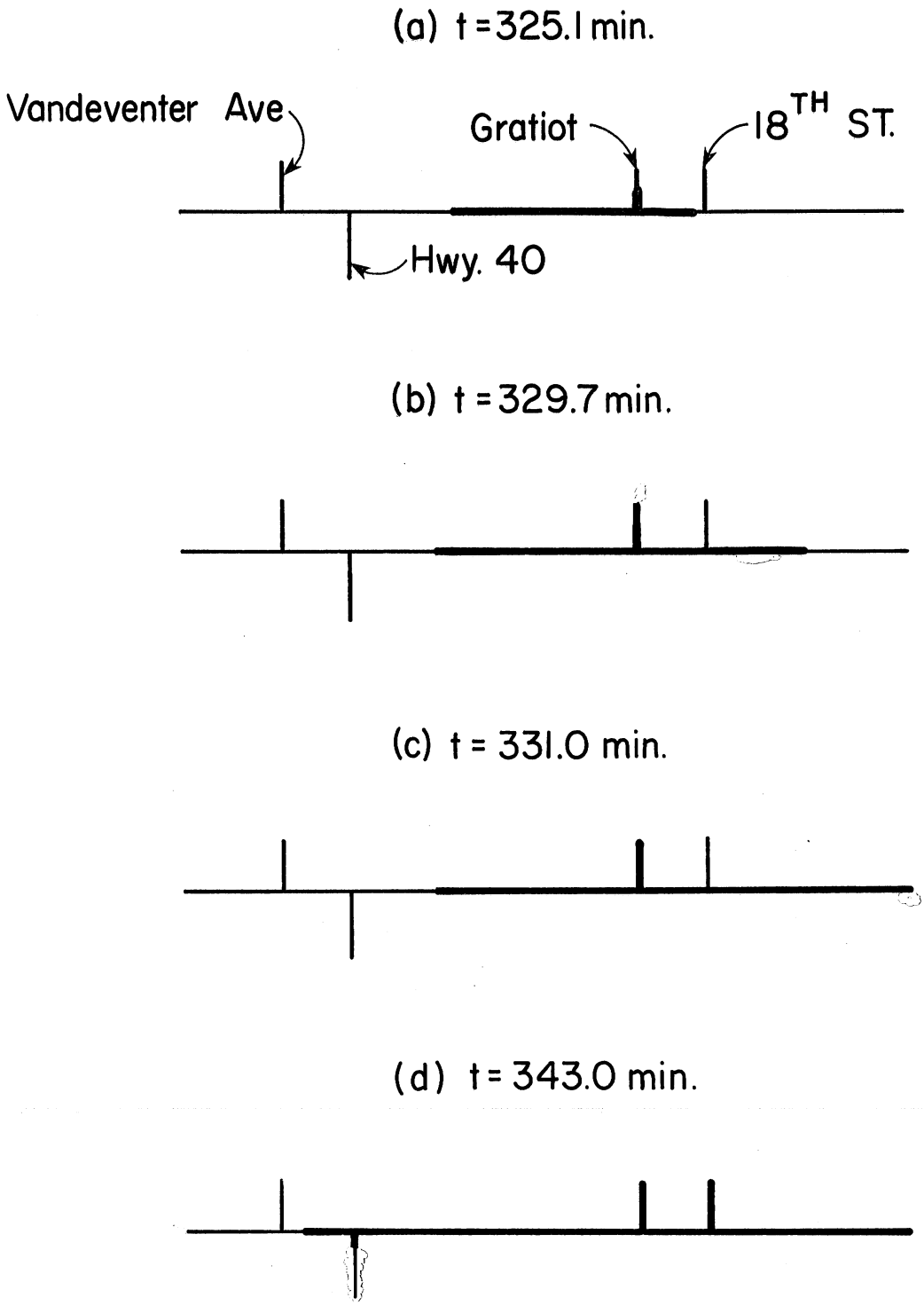

Fig. 14 - Pressurization Sequence for Run 5.

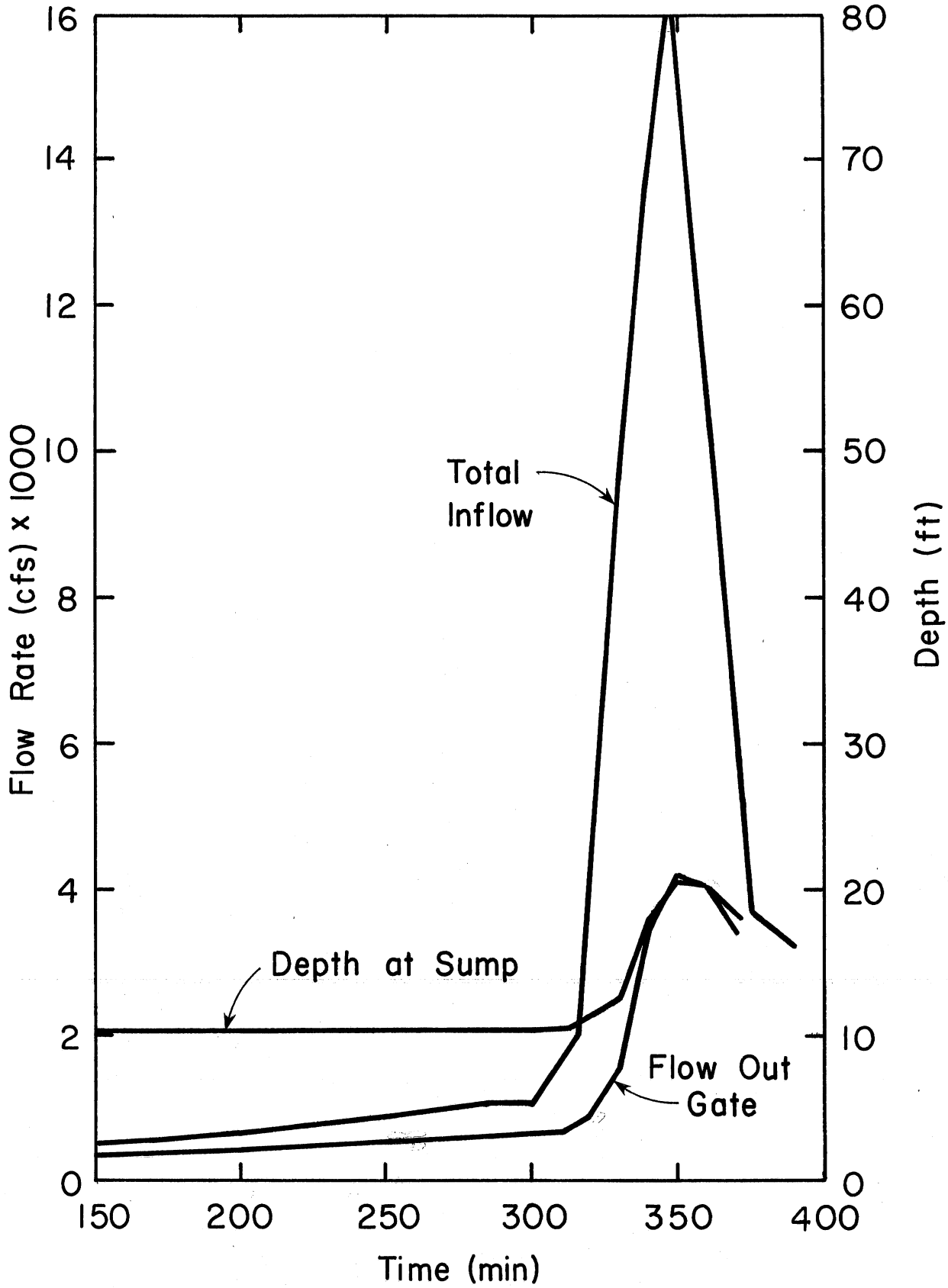

Fig. 15 - Hydrographs and Depth at Downstream End, Run 6, Old Mill Creek, 30 Year Storm, River Stage 17.4, Gate Controlled.

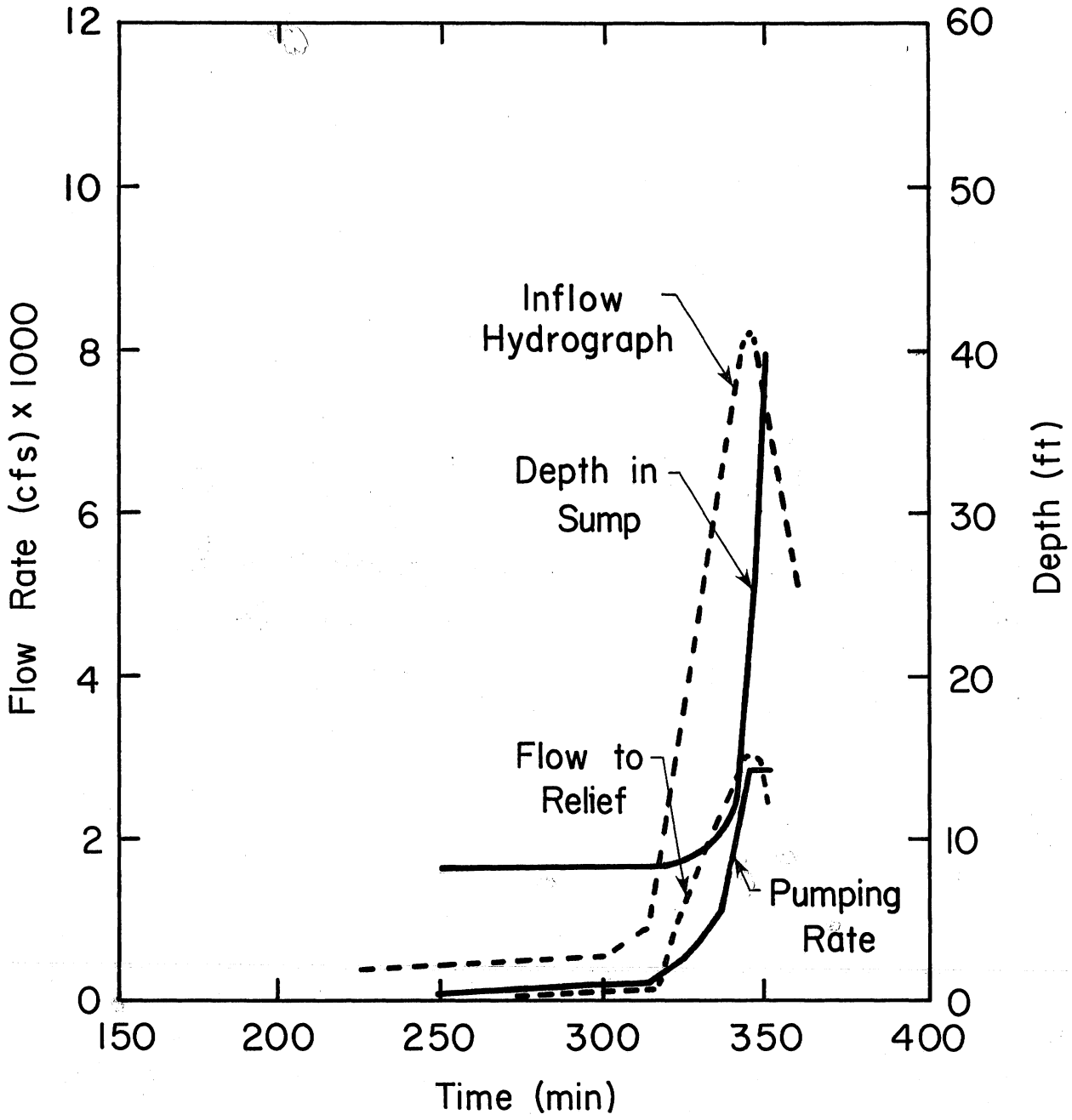

Fig. 16 - Hydrographs, Pumping Rate, and Depth, Run 7, Old Mill Creek, 1/2 x 30 Year Storm, Gate Closed.

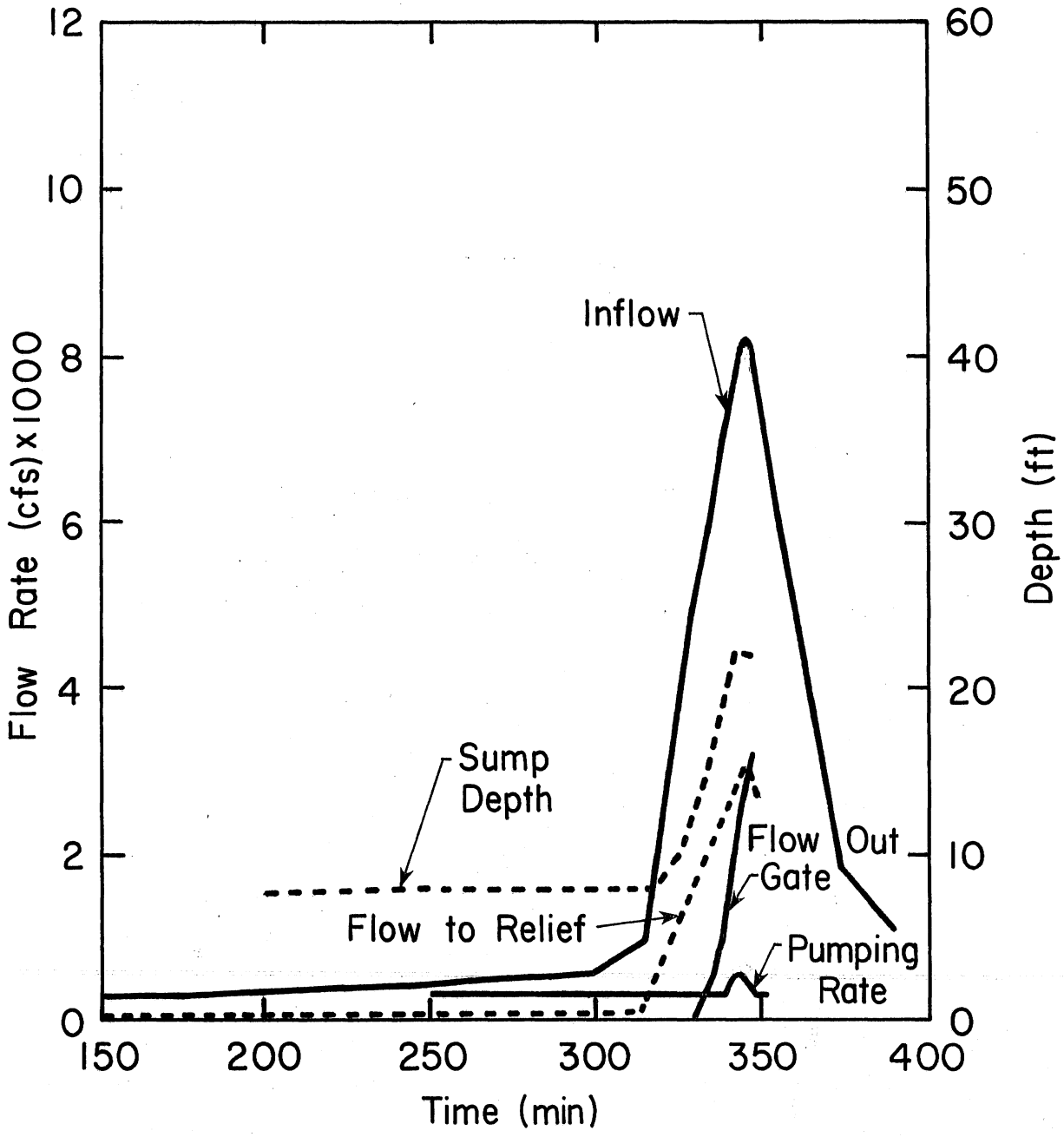

Fig. 17 - Hydrographs and Depth at Downstream End, Run 8, Old Mill Creek, 1/2 x 30 Year Storm, River Stage 26.

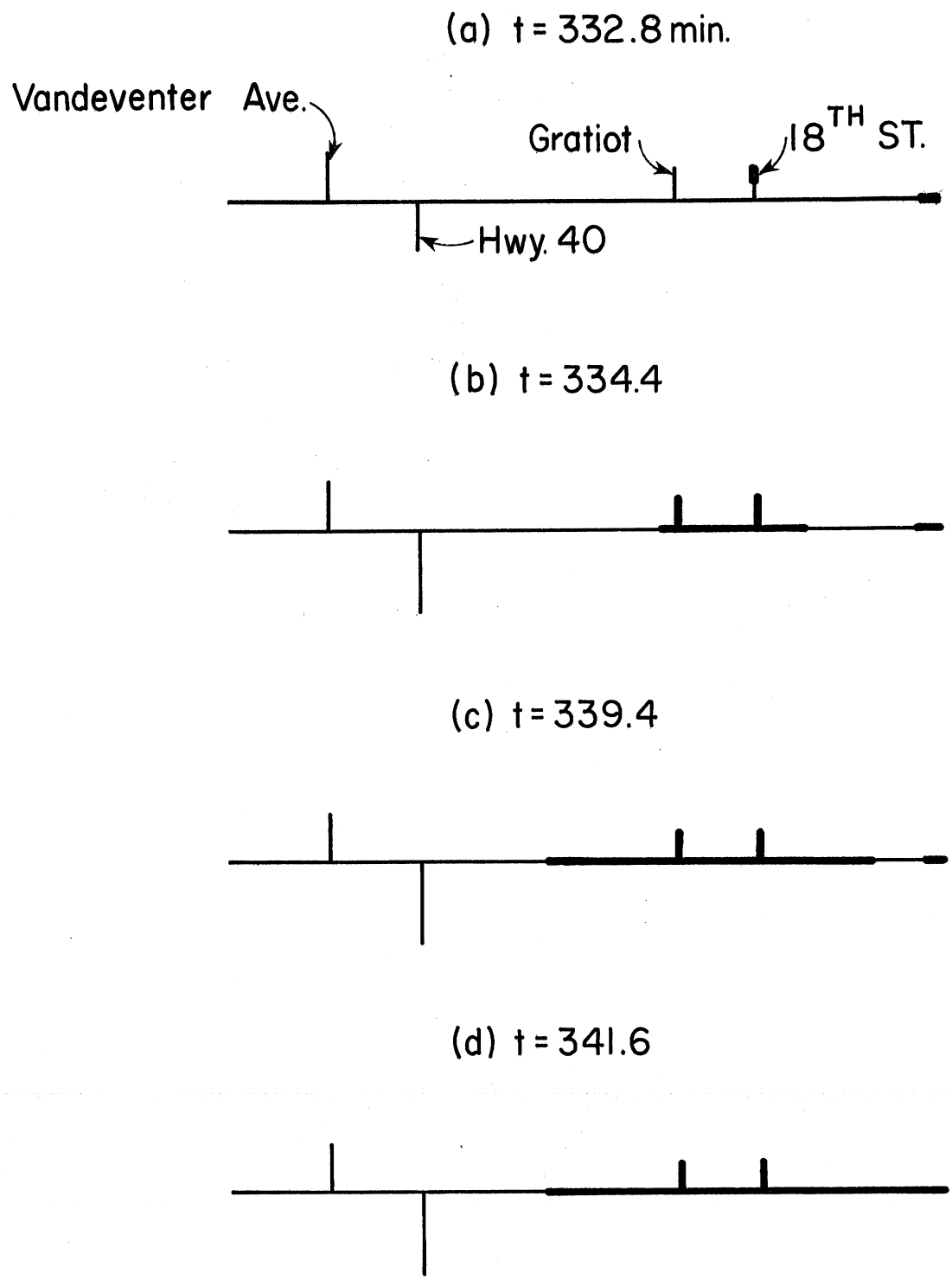

Fig. 18 - Pressurization Sequence for Run 8.

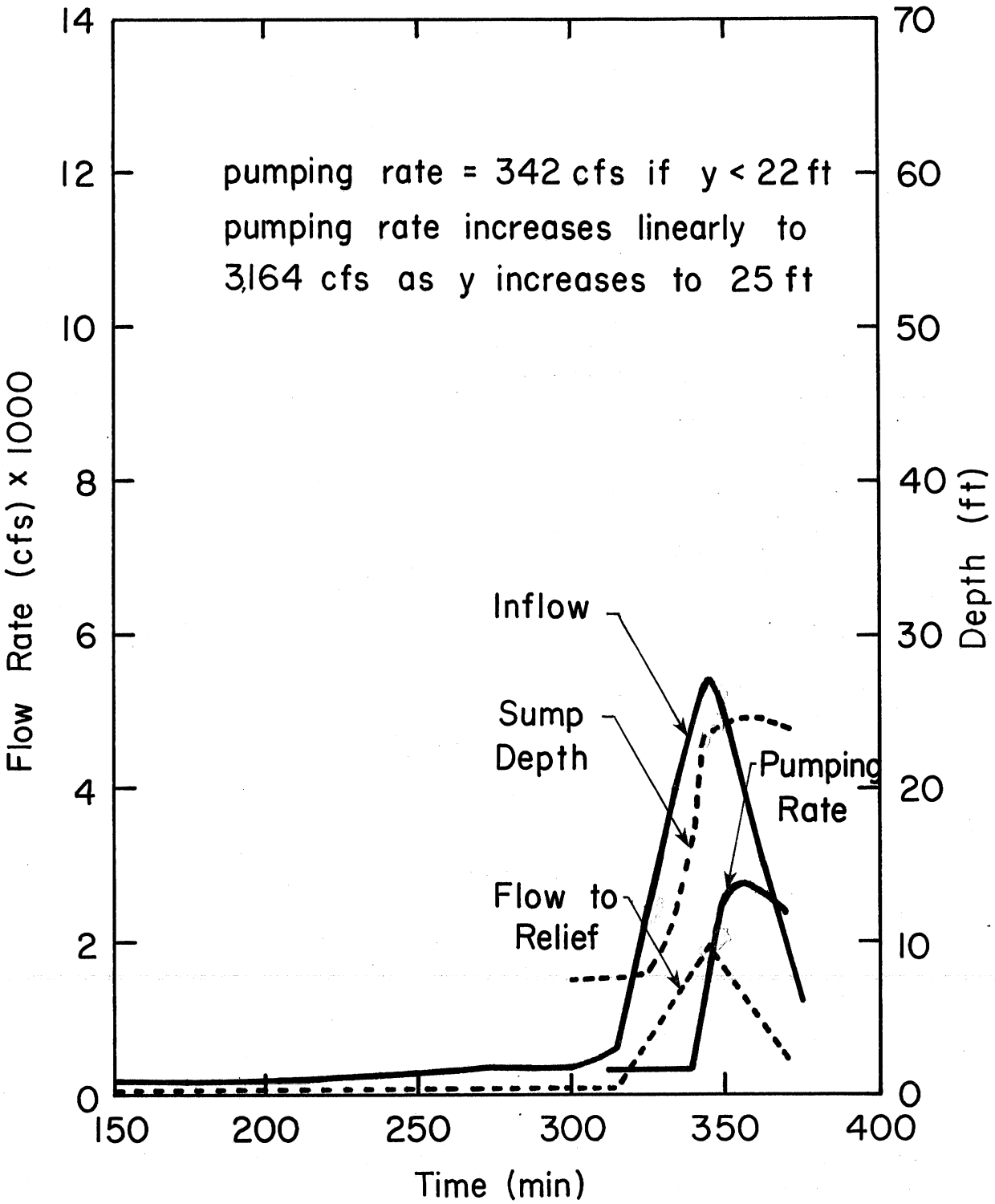

Fig. 19 - Hydrographs and Depth at Downstream End for Run 9, Old Mill Creek, 1/3 x 30 Year Storm, River Stage 32, Gate Closed.

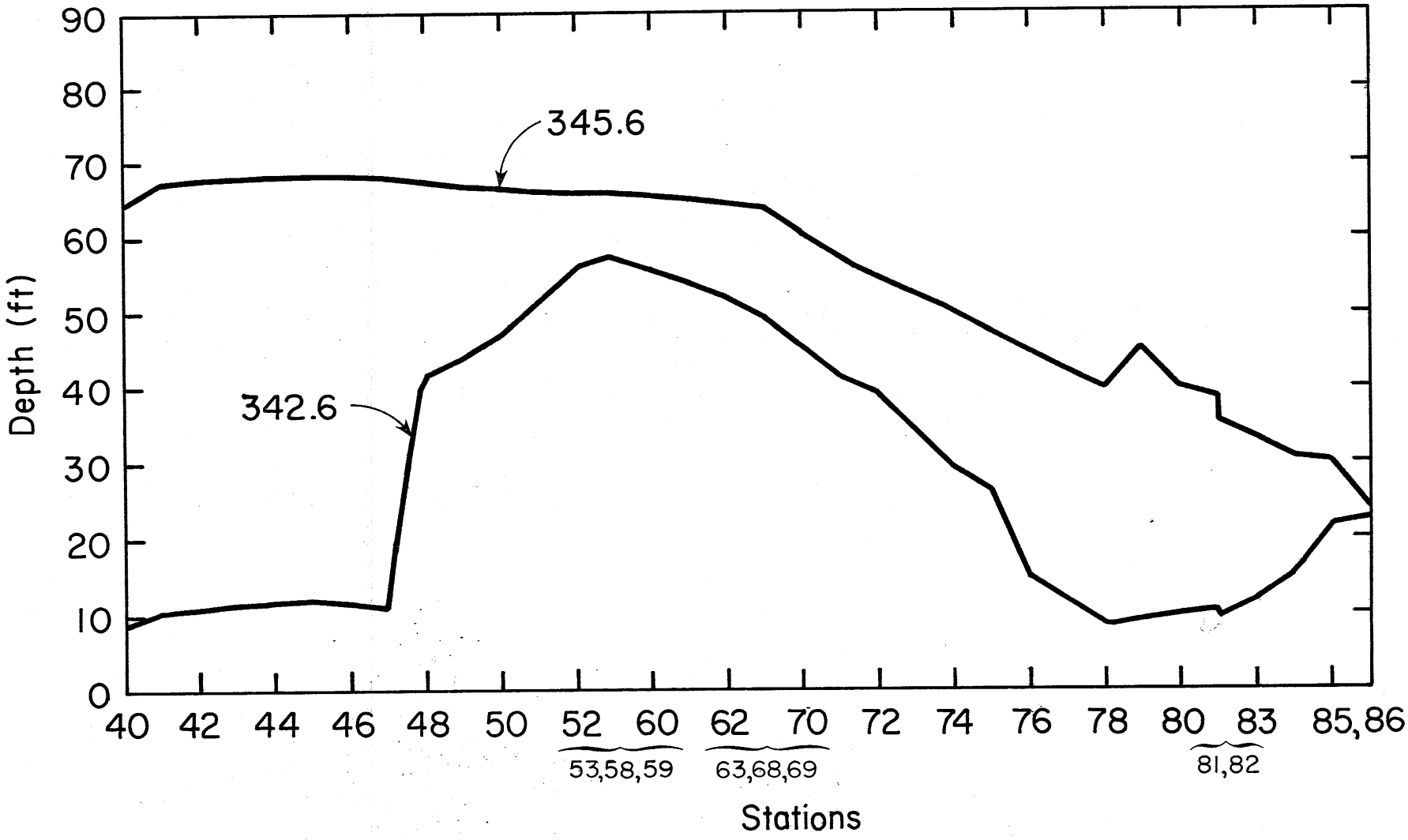

Fig. 20 - Hydraulic Grade Line After Pressurization, Run 9.

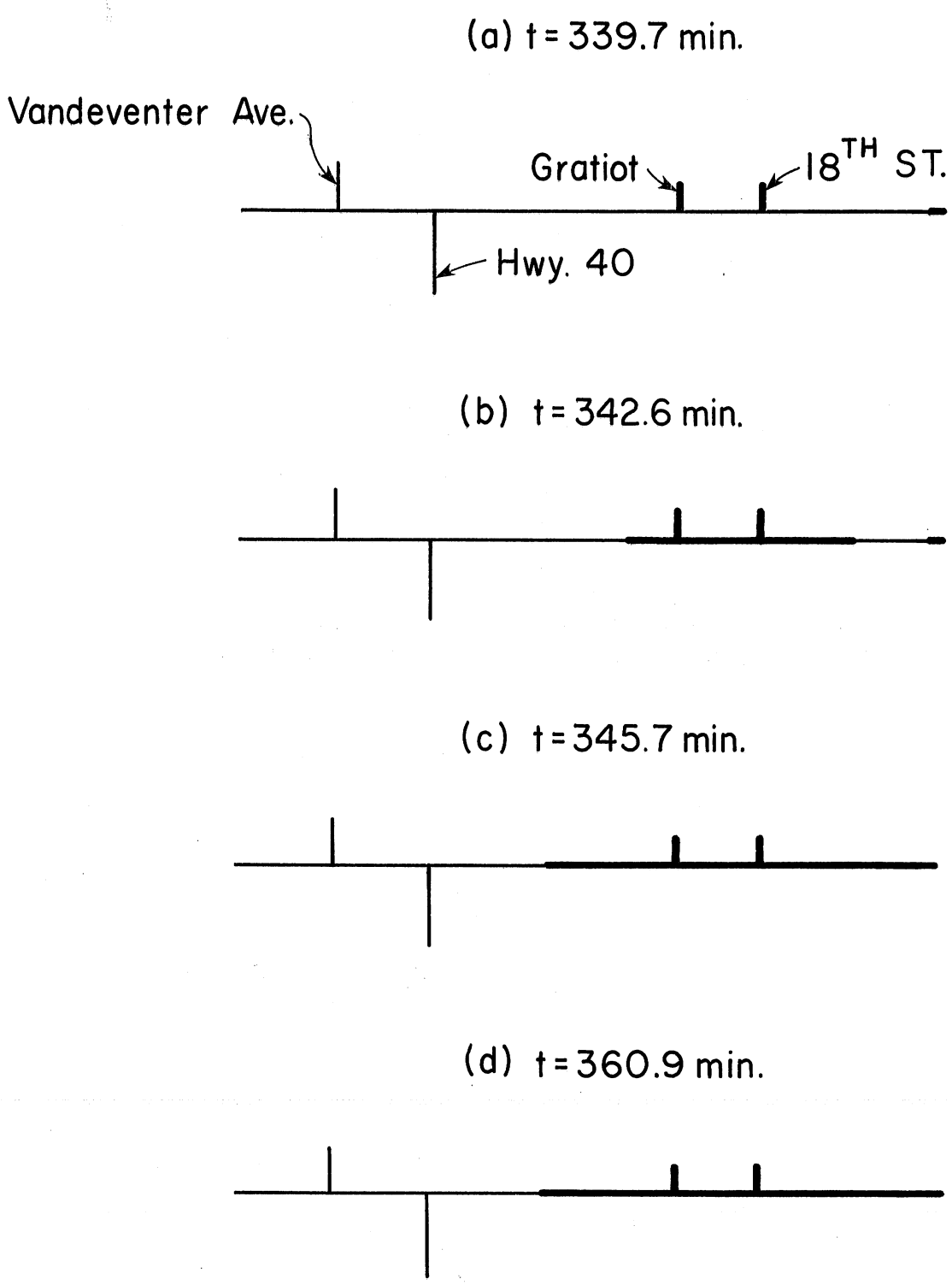

Fig. 21 - Pressurization Sequence for Run 9.

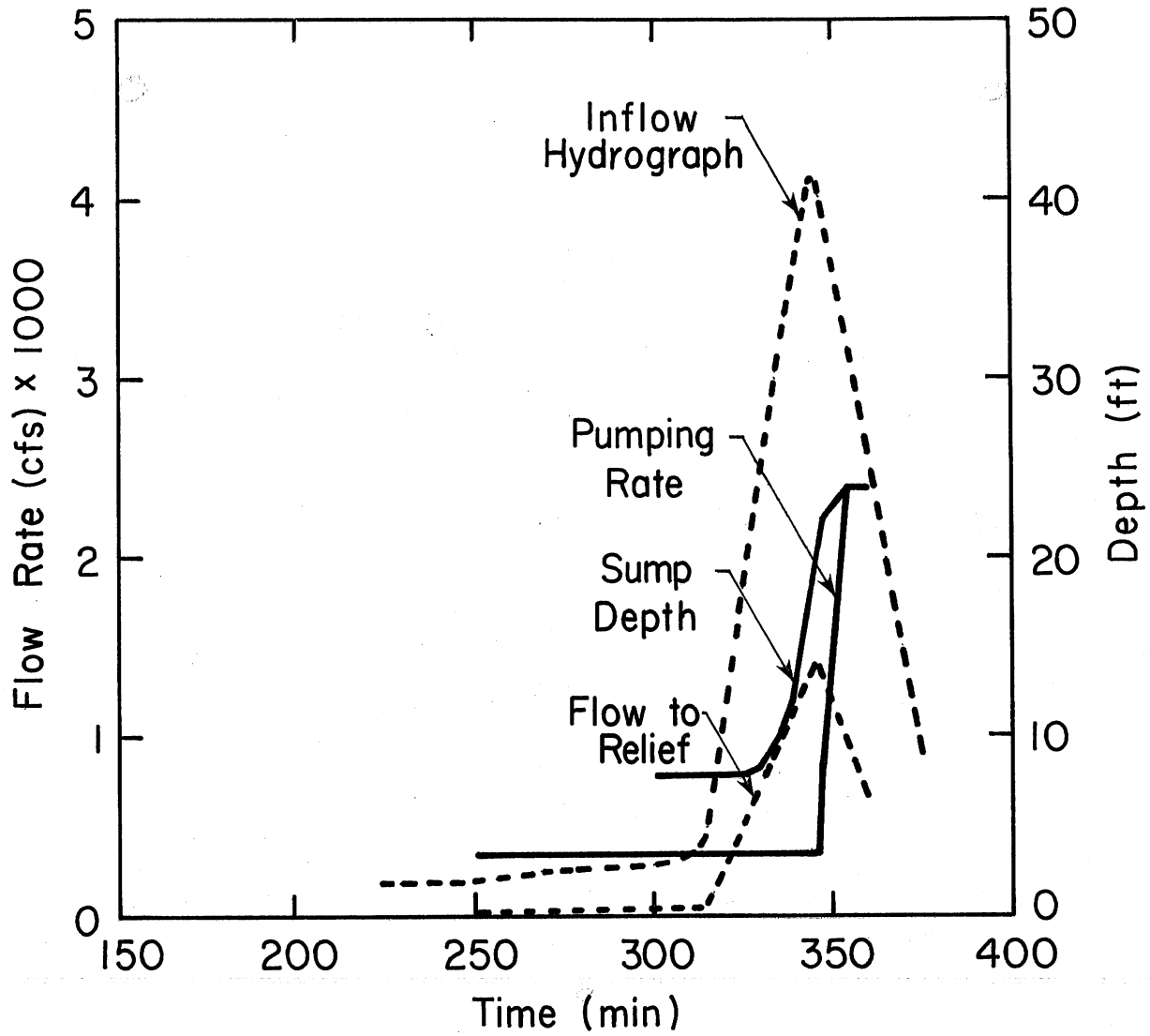

Fig. 22 - Hydrographs and Depth at Downstream End, Run 10, Old Mill Creek, 1/4 x 30 Year Storm, River Stage 32, Gate Closed.

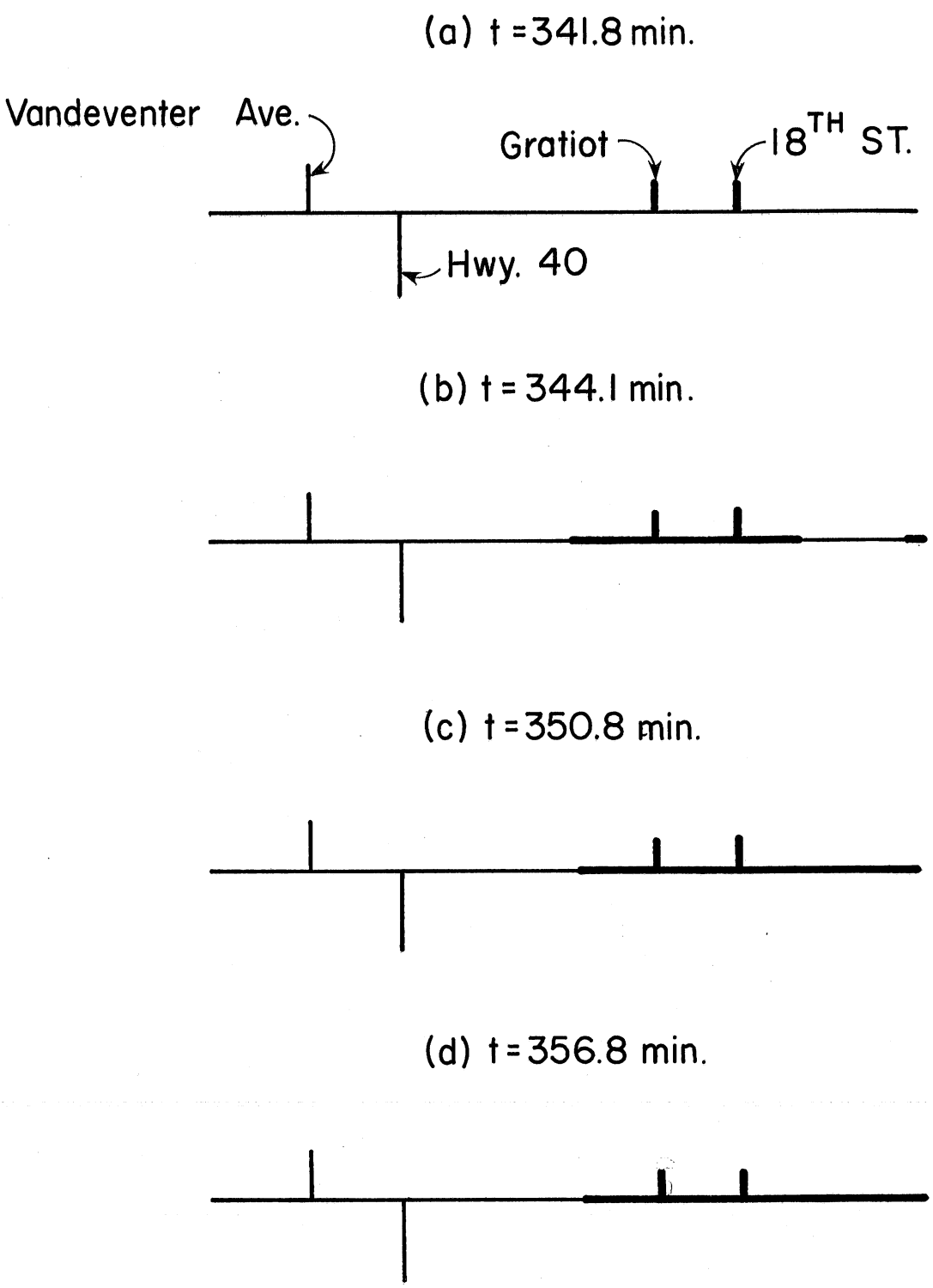

Fig. 23 - Pressurization Sequence for Run 10.

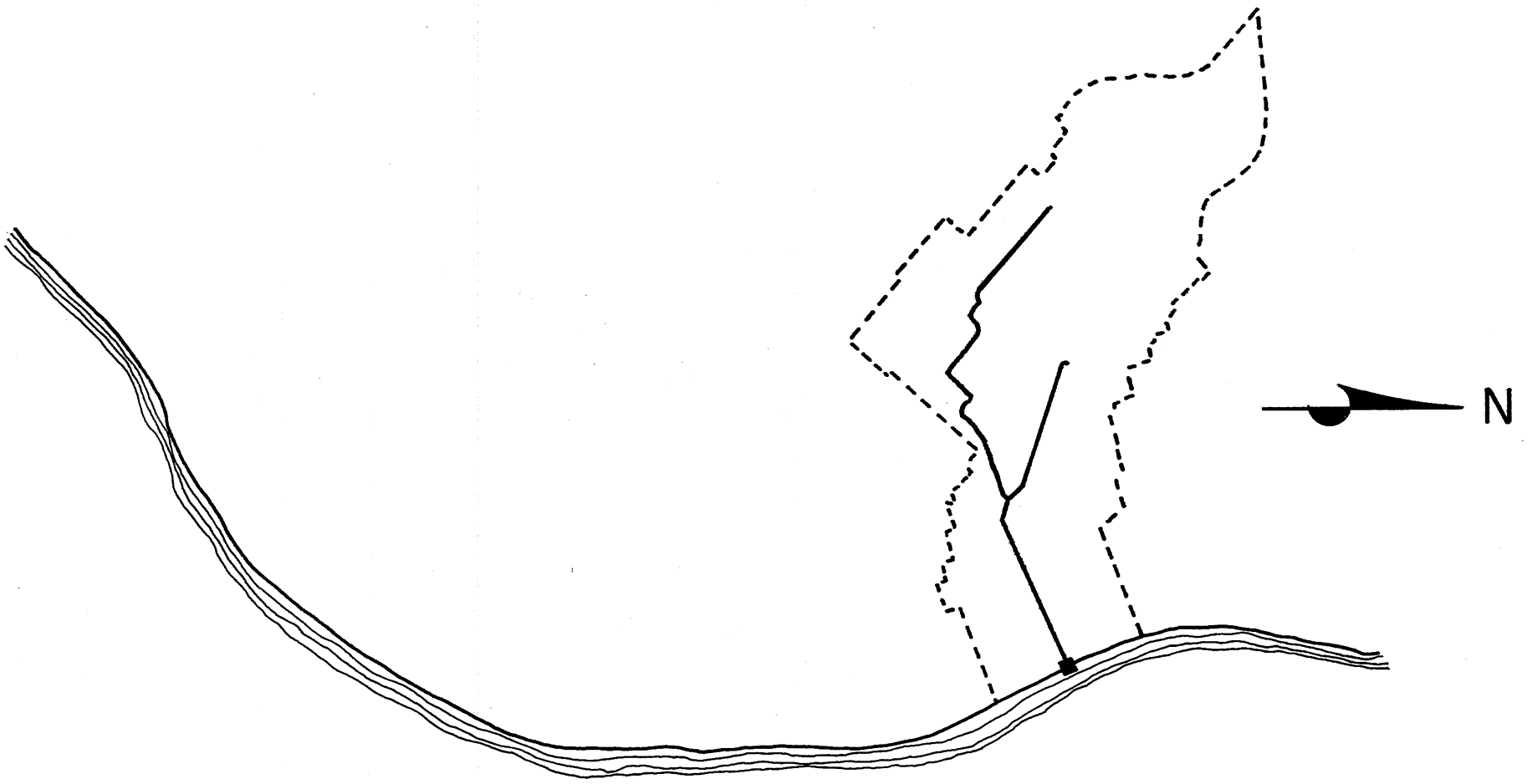

Fig. 24 - Maps Indicating Harlem Sewer System Modelled.

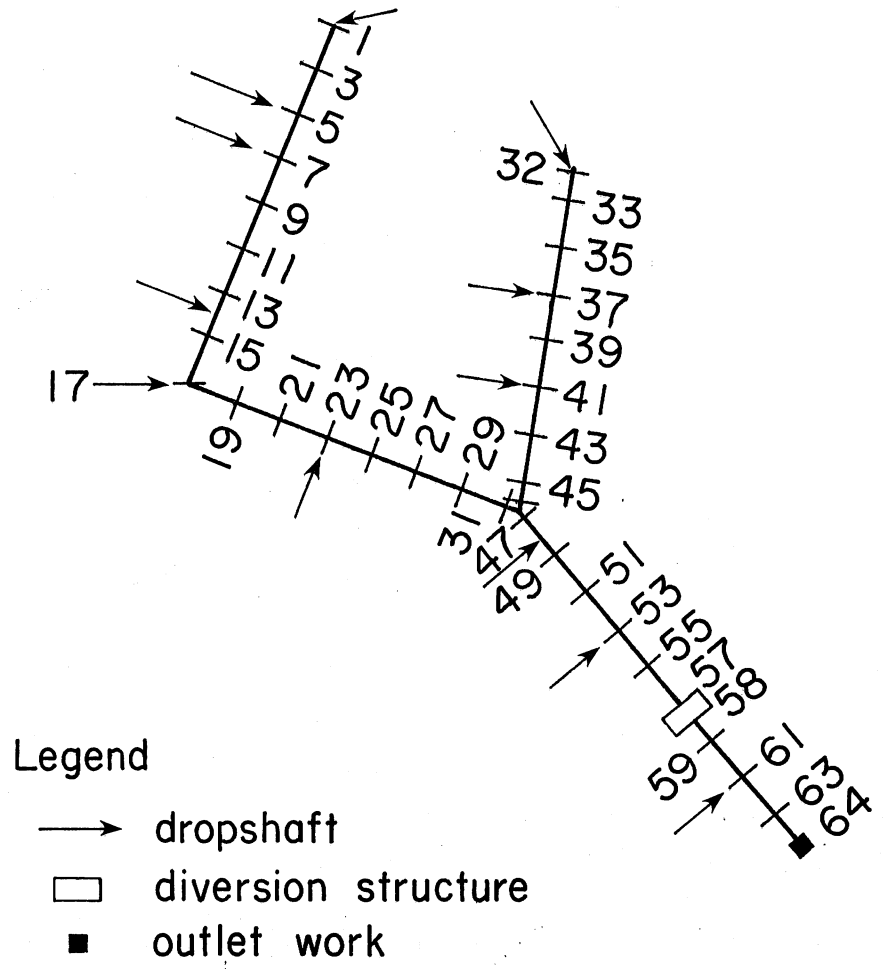

Fig. 25 - Harlem Sewer System Configuration.

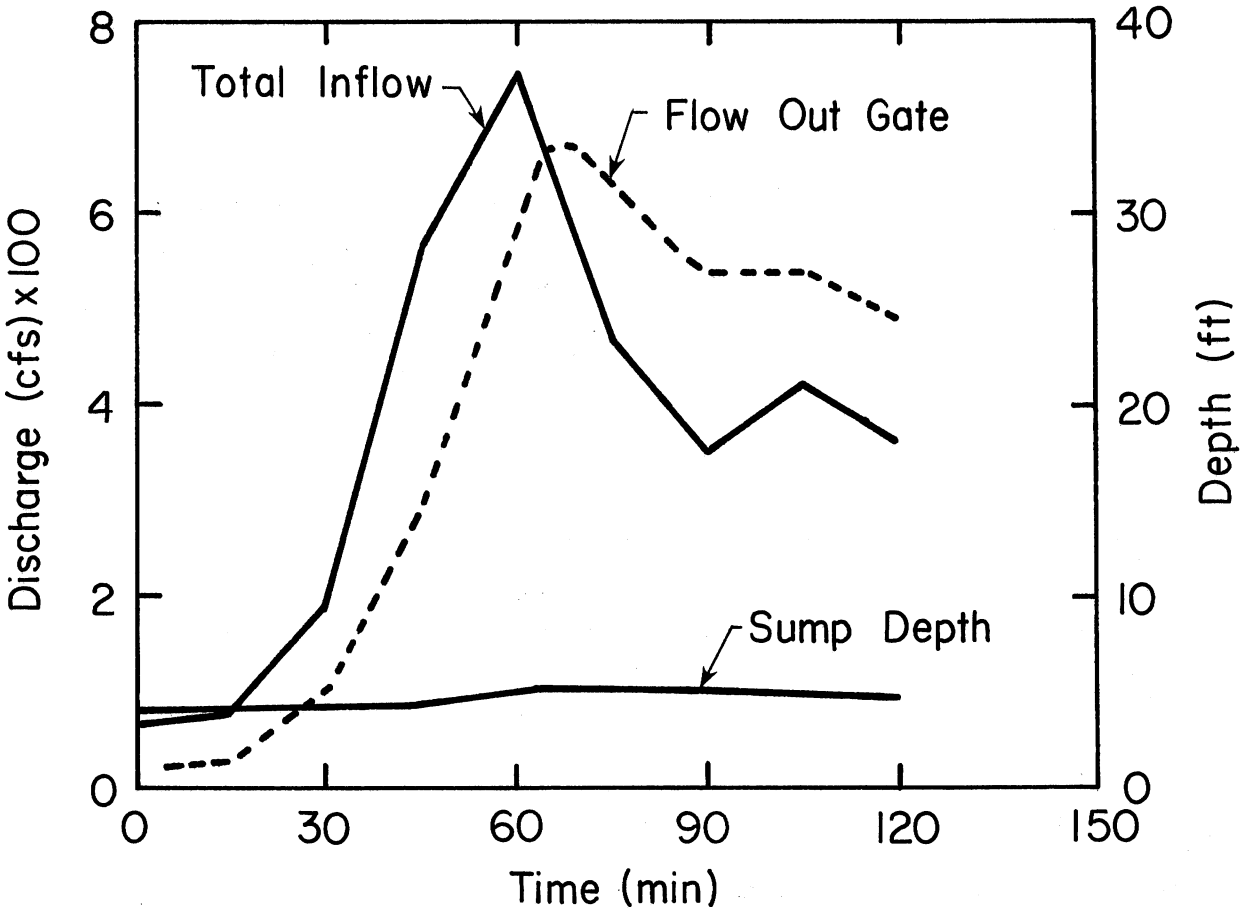

Fig. 26 - Hydrographs and Depth at Downstream End, Harlem, Typical Storm, River Stage 7.5 (Run 11).

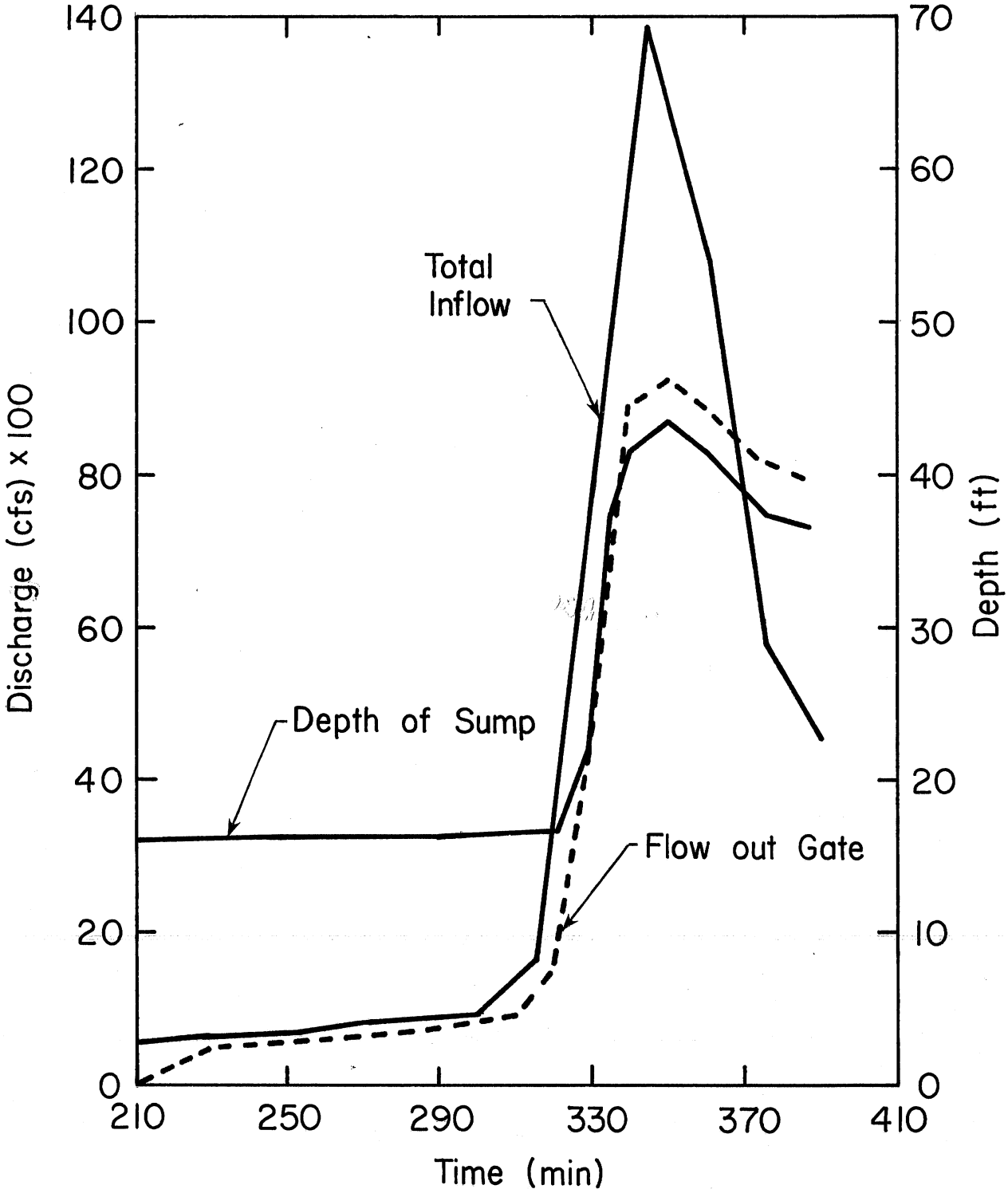

Fig. 27 - Hydrographs and Depth at Downstream End, Harlem, 30 Year Storm, River Stage 20.

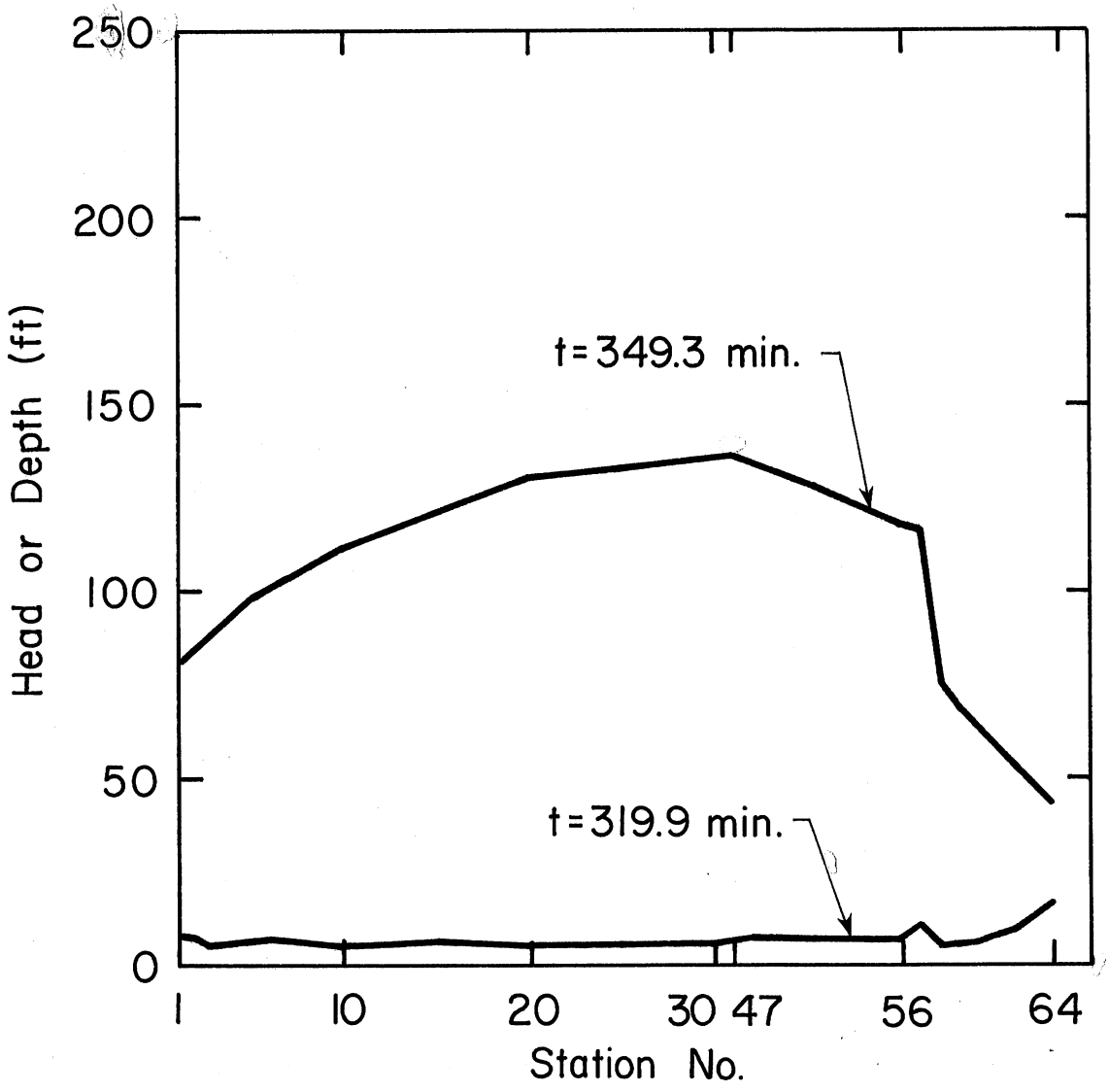

Fig. 28 - Typical Hydraulic Grade Lines, Harlem, 30 Year Storm, River Stage 20.

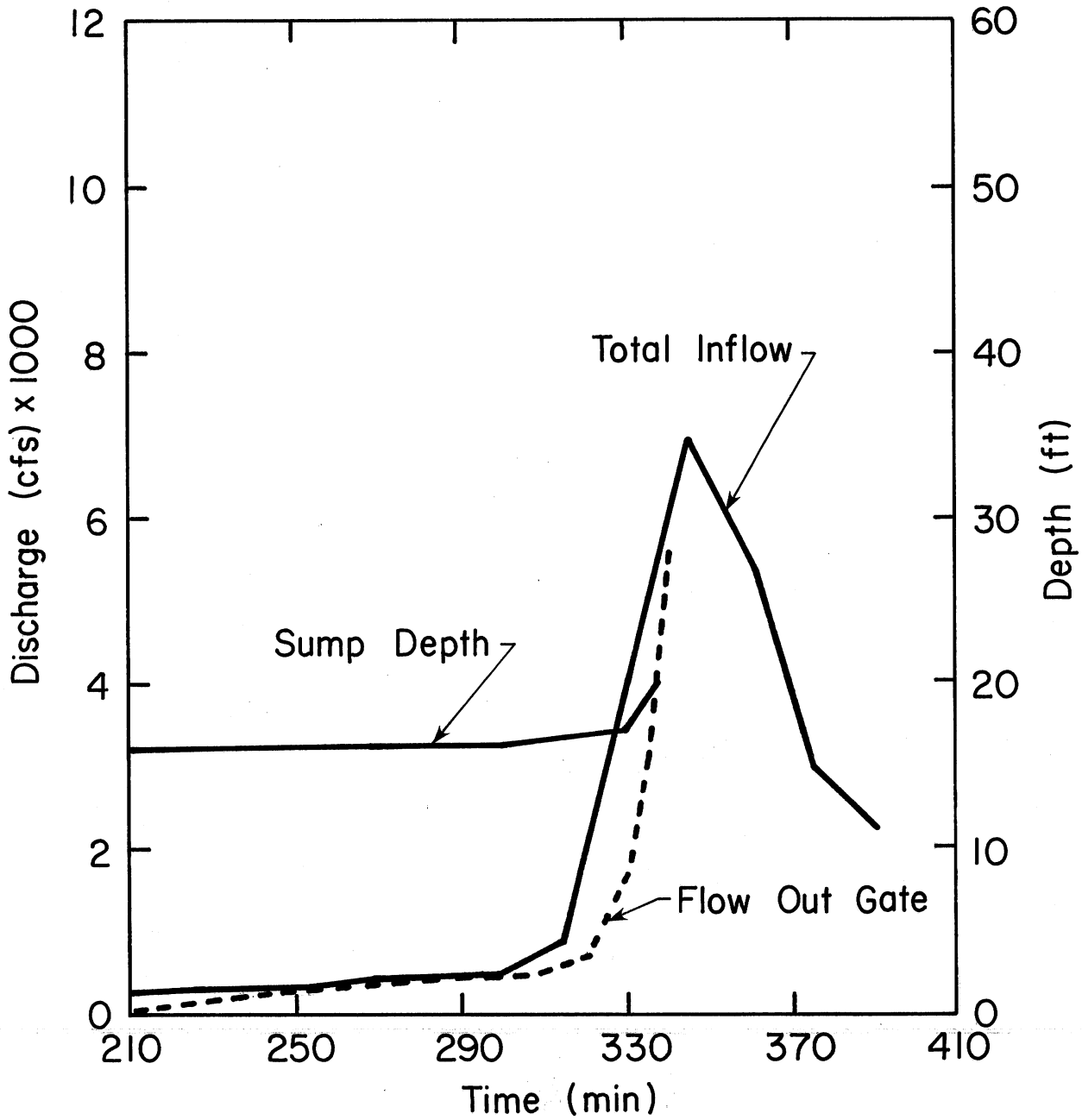

Fig. 29 - Hydrographs and Depth at Downstream End, Harlem, 1/2 x 30 Year Storm, River Stage 20 (Run 13).

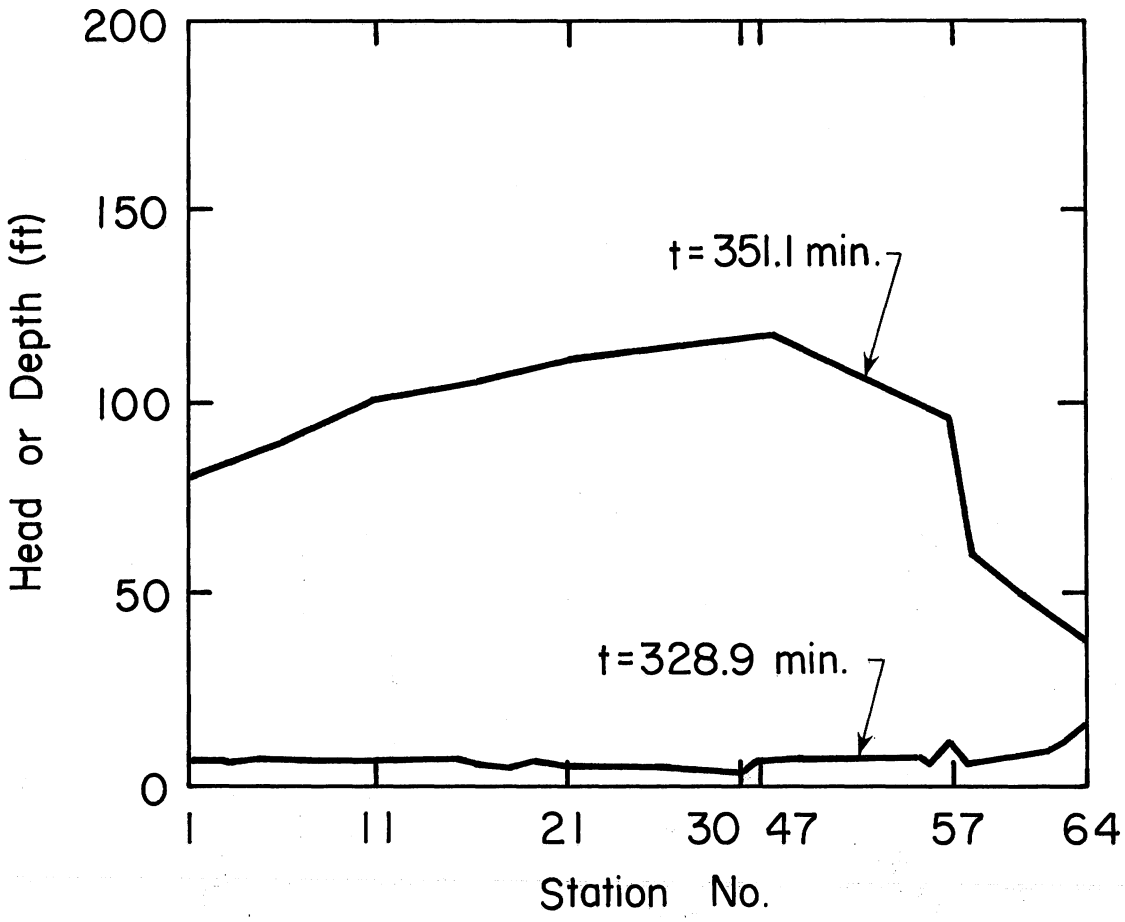

Fig. 30 - Typical Hydraulic Grade Lines, Harlem, 1/2 x 30 Year Storm, River Stage 20 (Run 13).

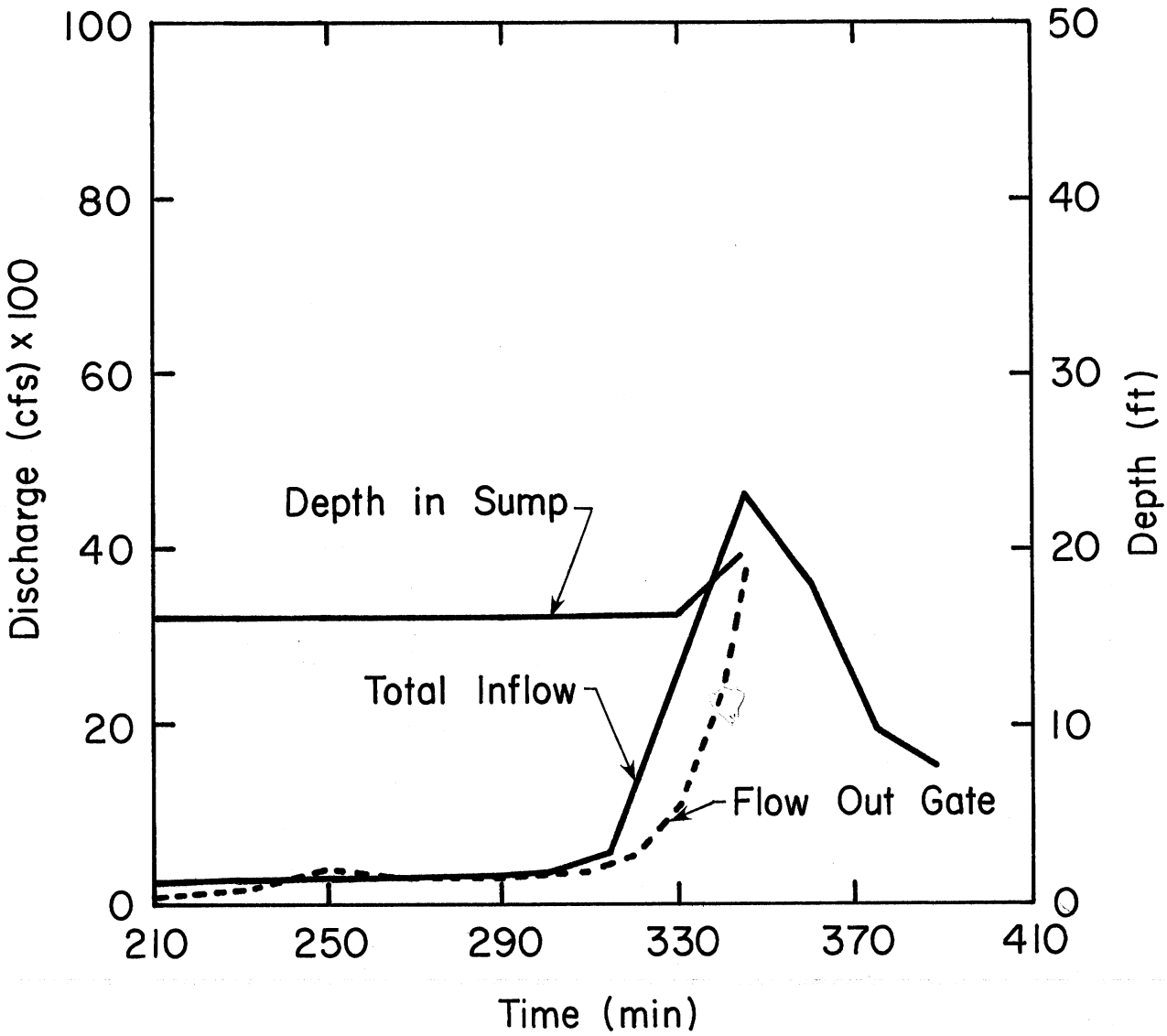

Fig. 31 - Hydrographs and Depth at Downstream End, Harlem, 1/3 x 30 Year Storm, River Stage 20 (Run 14).

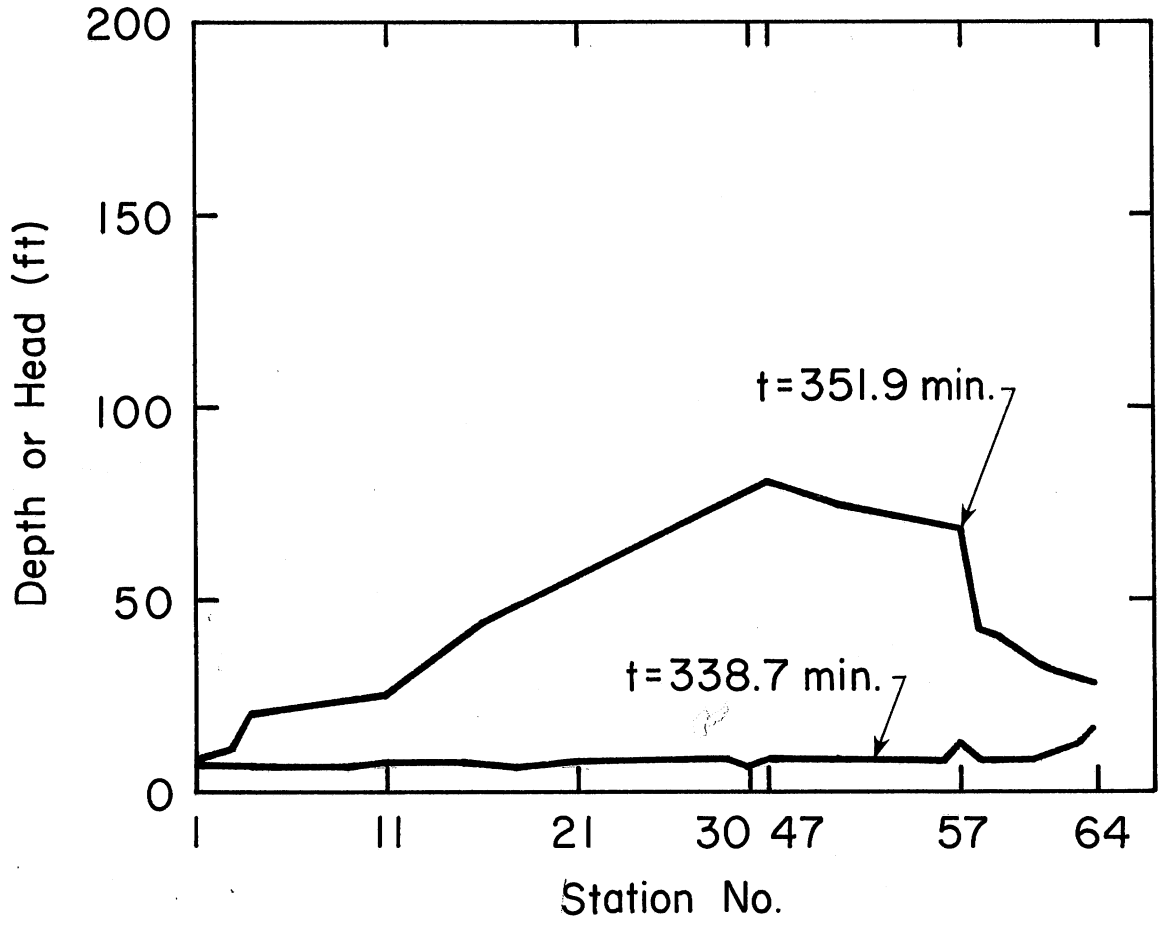

Fig. 32 - Typical Hydraulic Grade Lines, Harlem, 1/3 x 30 Year Storm, River Stage 20 (Run 14).

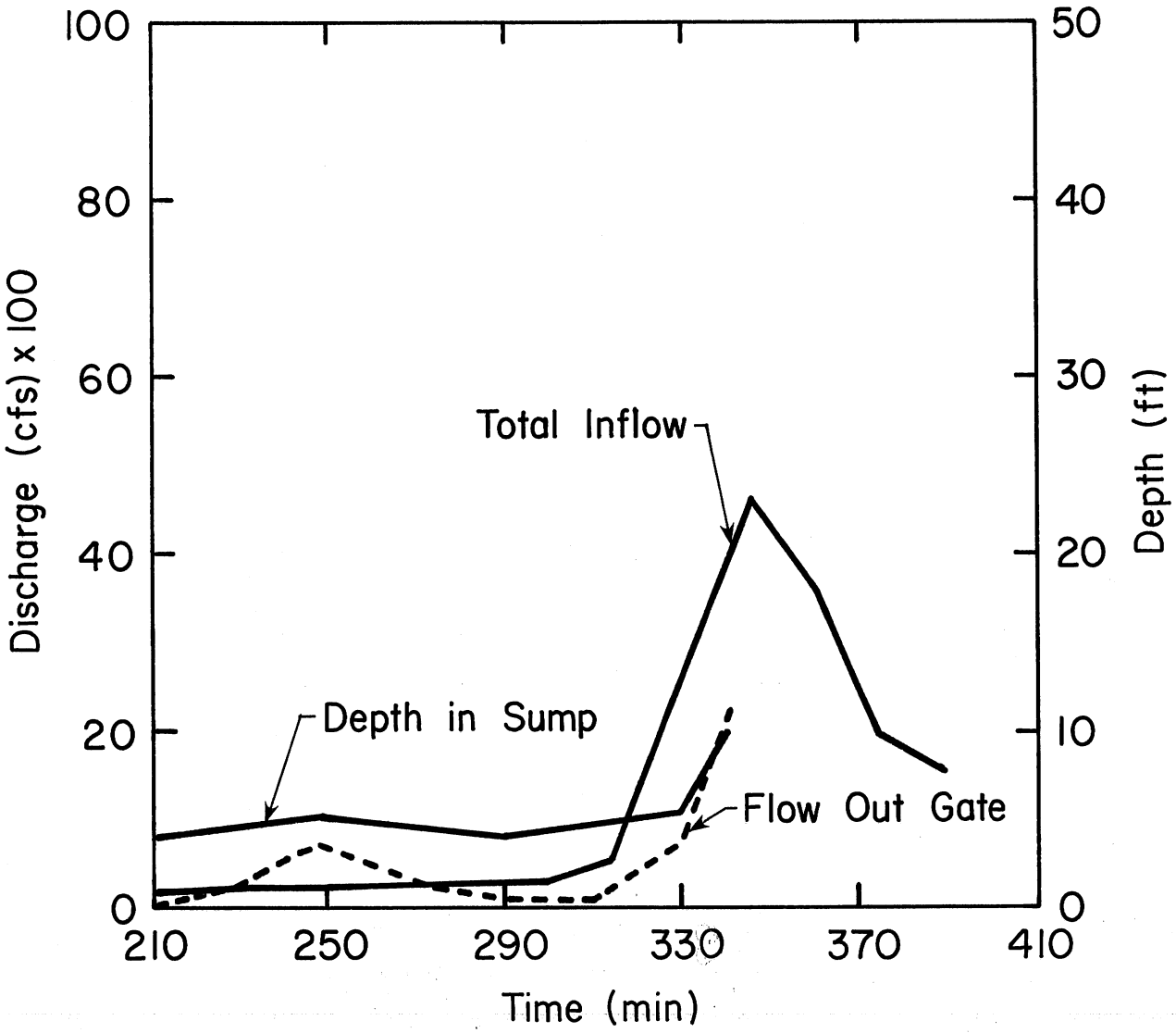

Fig. 33 - Hydrographs and Depth at Downstream End, Harlem, 1/3 x 30 Year Storm, River Stage 7.5 (Run 15).

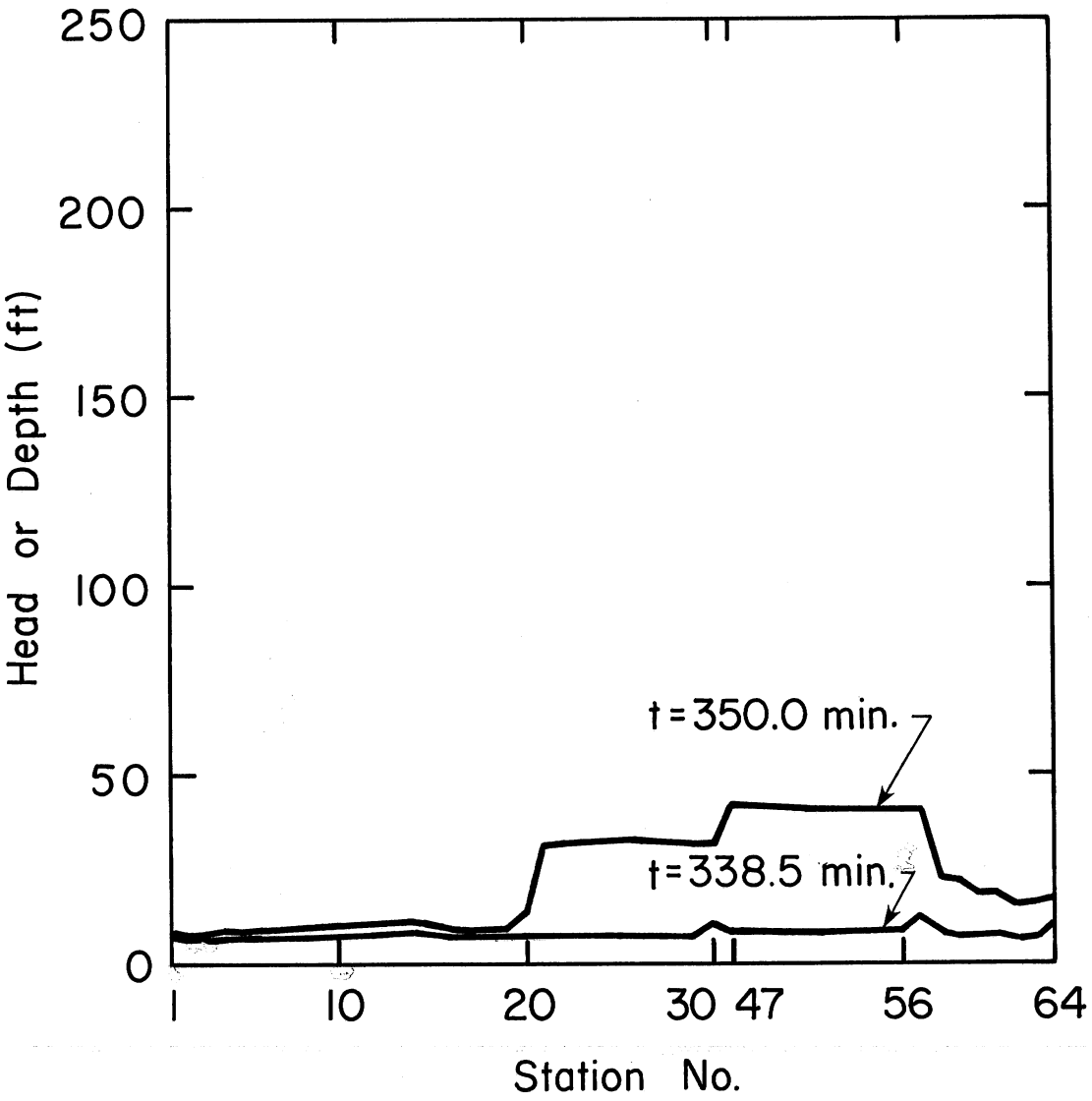

Fig. 34 - Typical Hydraulic Grade Line, Harlem, 1/3 x 30 Year Storm, River Stage 7.5 (Run 15).

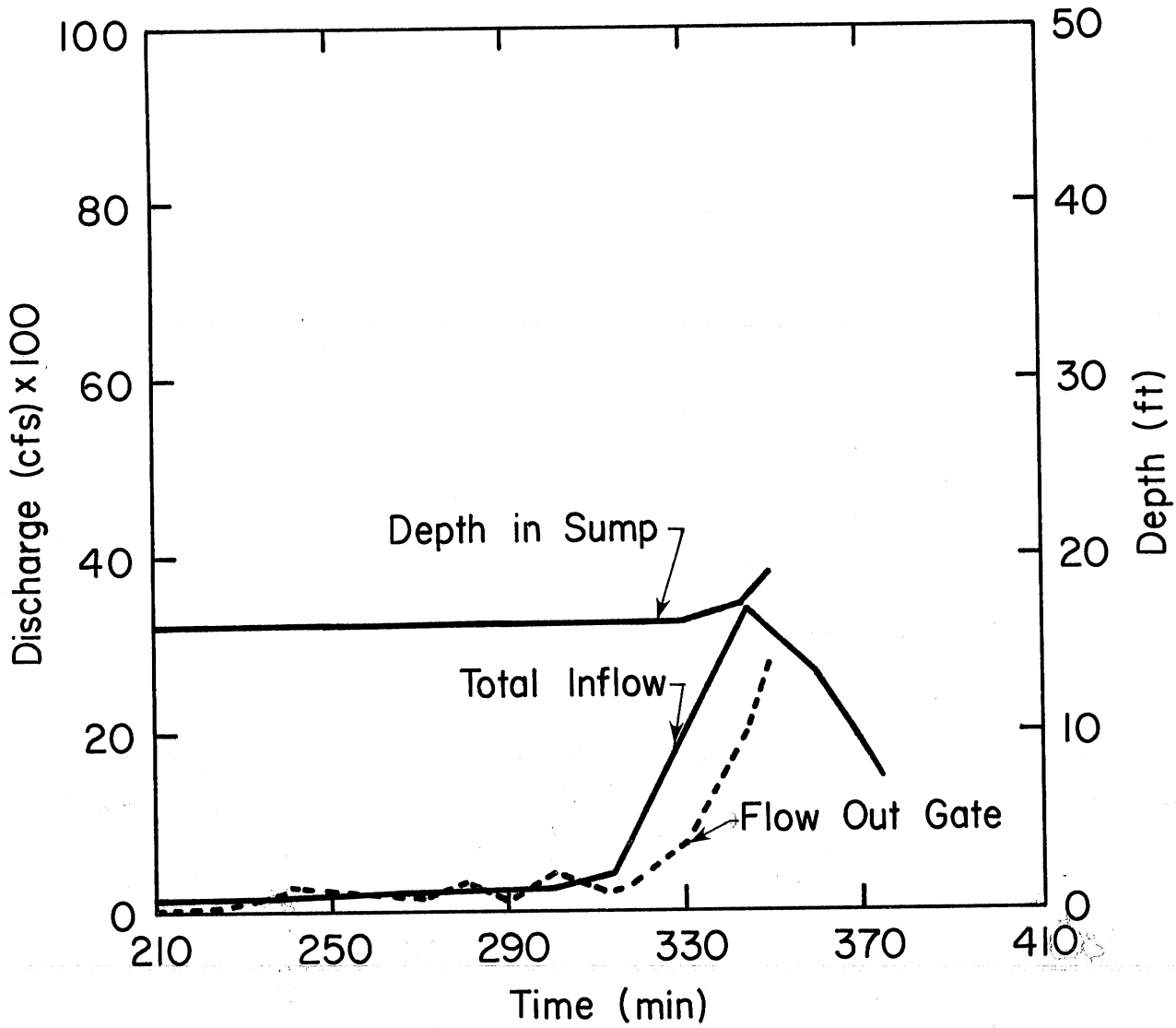

Fig. 35 - Hydrographs and Depth at Downstream End, Harlem, 1/4 x 30 Year Storm, River Stage 20, (Run 16).

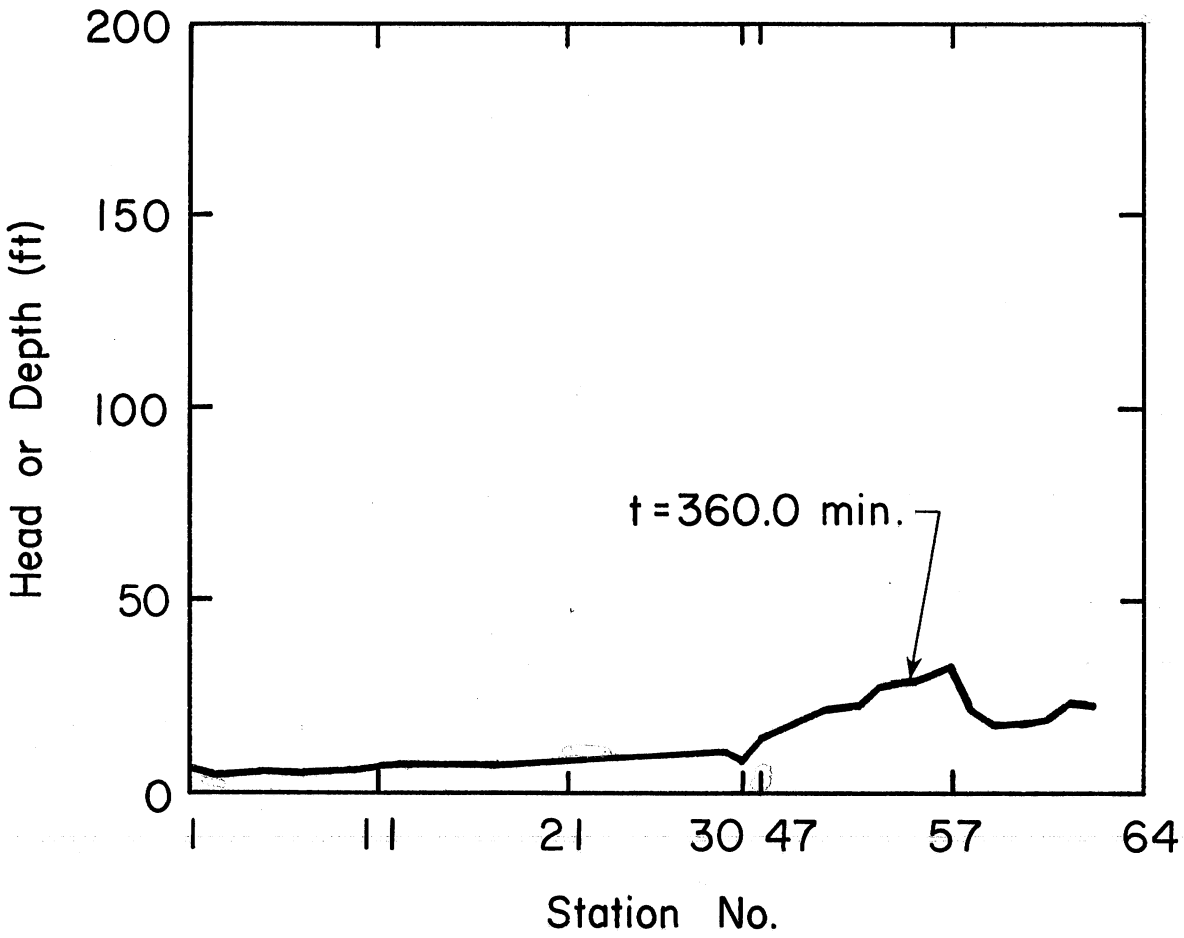

Fig. 36 - Typical Hydraulic Grade Line Near Peak Discharge, Harlem, 1/4 x 30 Year Storm, River Stage 20, (Run 16).

APPENDIX

APPENDIX

Description of the Mathematical Model

General

This mathematical model is based on the full equations of continuity and motion (St. Venant equations) applicable to one dimensional unsteady flows in open channel and closed conduits. The governing equations for open channel flow are

$$\frac{\partial y}{\partial t} + V\frac{\partial y}{\partial x} + \frac{c^2}{g}\frac{\partial V}{\partial x} = 0 \qquad \text{(A-1)}$$

and

$$g\frac{\partial y}{\partial x} + \frac{\partial V}{\partial t} + V\frac{\partial V}{\partial x} + g(s_f - s_o) = 0 \qquad \text{(A-2)}$$

in which c is the gravity wave speed given by

$$c = \sqrt{\frac{gA}{T}} \qquad \text{(A-3)}$$

The corresponding equations for closed conduit flow are

$$\frac{\partial H}{\partial t} + V\frac{\partial H}{\partial x} + \frac{a^2}{g}\frac{\partial V}{\partial x} = 0 \qquad \text{(A-4)}$$

and

$$g\frac{\partial H}{\partial x} + \frac{\partial v}{\partial t} + V\frac{\partial v}{\partial x} + g(s_f - s_o) = 0 \qquad \text{(A-5)}$$

in which a is the speed of the pressure wave.

The following is a list of the symbols used in the above equations:

y = depth of flow
V = velocity of flow,
H = piezometric head
g = acceleration due to gravity,
A = area of flow
T = top width of flow

Appendix (Cont.)

s_f = friction slope, s_o = slope of channel or pipe

t = time, x = distance measured along channel or pipe

There are a number of different approaches available for solving the above differential equations, but in view of the complex geometrical configuration to be dealt with, the method of characteristic appears to be the most suitable. The characteristic equations are, for open channel flow,

$$\frac{dx}{dt} = V \pm C \tag{A-6}$$

$$\frac{dy}{dt} \pm \frac{C}{g}\frac{dV}{dt} \pm C(s_f - s_o) = 0 \tag{A-7}$$

and for closed conduit flow

$$\frac{dx}{dt} = V \pm a \tag{A-8}$$

$$\frac{dH}{dt} \pm \frac{a}{g}\frac{dV}{dt} \pm a(s_f - s_o) = 0 \tag{A-9}$$

Note that the two sets of characteristic equations have identical forms. For the characteristic method to converge, the following stability criteria must be enforced.

Open Channel Flow $\quad \Delta t \leq \Delta x/|V \pm C|$ (A-10)

Closed Conduit Flow $\quad \Delta t' \leq \Delta x/|V \pm a|$ (A-11)

When mesh sizes are chosen according to the above stability criteria, the characteristic lines issuing from a nodal point P will intersect the line representing the previous time, as shown in Fig. A-1, provided that the

Appendix (Cont.)

flow is subcritical. These intersects are denoted R and S in Fig. A-1. Accordingly, the characteristic differential equations, Eqs. (A-7) and (A-9), can be written as:

for open channel flows,

$$C^+ : y_P - y_R + \frac{C_R}{g}(V_P - V_R) + C_R(S_f - S_o)_R \ \Delta t = 0 \qquad \text{(A-12)}$$

$$C^- : y_P - y_S - \frac{C_S}{g}(V_P - V_S) - C_S(S_f - S_o)_S \ \Delta t = 0 \qquad \text{(A-13)}$$

and for closed conduit flows,

$$C^+ : H_P - H_R + \frac{a}{g}(V_P - V_R) + a(S_f - S_o)_R \ \Delta t' = 0 \qquad \text{(A-14)}$$

$$C^- : H_P - H_S - \frac{a}{g}(V_P - V_S) - a(S_f - S_o)_S \ \Delta t' = 0 \qquad \text{(A-15)}$$

When the flow at the nodal points, A, B, and C is known, then the corresponding values at the intersects R and S can be obtained by linear interpolations. In principle, a set of unknowns (Y_P, V_P) or (H_P, V_P) can be readily obtained by solving Eqs. (A-12) and (A-13) or Eqs. (A-14) and (A-15), respectively.

Computation at the interface requires a special treatment. According to Eq. (A-3), $c \to \infty$ as $T \to o$. To overcome this physically unrealistic situation, Song (1976) assumed that the phase change will occur at a depth slightly less than the diameter D so that the flow is regarded as open channel when

$$y \leq D - \varepsilon \qquad \text{(A-16)}$$

but closed conduit when

$$y \geq D - \varepsilon \qquad \text{(A-17)}$$

Appendix (Cont.)

Assuming that the interface is originally located at point C in Fig. A-2 and moving to the left at speed W, the new location of the interface after $\Delta t'$ is indicated by point p'. The distance moved is

$$x' = W\ t' \tag{A-18}$$

Since there is a jump in the depth of ε across the interface, there is also a jump in V across the interface. The depth just upstream of the interface is assumed to be $D - \varepsilon$. The head just downstream of the interface, Hp2, the velocity just upstream of the interface, Vp1, and the velocity just downstream of the interface, Vp2, are unknowns. There are a total of four unknowns at the interface, including W. There are available two characteristic equations corresponding to $\overline{p'R}$ and $\overline{p'S}$ characteristic lines. In addition, it is possible to write a continuity equation across the jump as

$$(VP1 + W)A_1 = (VP2 + W)A_2 \tag{A-19}$$

where A_1 and A_2 are the known cross-sectional areas. The momentum equation across the interface is

$$F_1 - F_2 = \rho(VP1 + W)A_1\ (VP2 - VP1) \tag{A-20}$$

where F_1 is the force due to hydrostatic pressure in the flow depth $D - \varepsilon$ and F_2 is the force due to the head of Hp2 in closed conduit. There are four equations and four unknowns at the interface, assuming ε is given.

Boundary Conditions

There are many abrupt changes in sizes and shapes, junctions, and flow control structures, etc. where special boundary conditions are required. A few typical boundary conditions are described below.

Appendix (Cont.)

1. Upstream End

At an upstream end it is generally assumed that the discharge is equal to a known runoff hydrograph previously computed. That is

$$Q = Q(t) \tag{A-21}$$

This equation plus a negative characteristic equation, either Eq. (A-13) or Eq. (A-15), provides the necessary equations for the determination of the two unknowns.

2. Expansion or Contraction

A typical expansion joint is sketched in Fig. A-3. Since there is an abrupt change in the flow across the joint, the joint is represented by two stations, C1 and C2. There are four unknowns, Y_{p1} (H_{p1}), V_{p1}, y_{p2} (H_{p2}), and V_{p2}. Two characteristic equations are available - the C+ equation for station 1 and C- equation for station 2. The two additional equations required are the continuity equation

$$V_{p1} A_{p1} = V_{p2} A_{p2} \tag{A-22}$$

and a fairly common assumption that the piezometric head is unchanged between station 1 and station 2. That is

$$H_{p1} = H_{p2},\ y_{p1} = y_{p2},\ \text{or}\ H_{p1} = y_{p2} \tag{A-23}$$

whichever may be appropriate. Althouth it is possible to specify the expansion loss in lieu of Eq. (A-23), this equation is simpler and produces satisfactory results.

3. 3-Way Junction

A typical horizontal 3-way junction is shown in Fig. A-4. This junction is represented by three stations and six unknowns. The required equations are the three characteristic equations, the continuity equation

Appendix (Cont.)

$$V_{p1} A_{p1} + V_{p2} A_{p2} = V_{p3} A_{p3} \qquad \text{(A-24)}$$

and the assumption that the heads are equal at the three stations.

4. Dropshaft Inlet

There are a number of different flow conditions possible at a dropshaft, but only two simple cases are shown in Fig. A-5. Sketch (a) indicates the open channel condition at the dropshaft with known point input Q(t). There are three unknowns, V_{p1}, V_{p2}, and y_p. Two characteristic equations are available. The third equation is furnished by the continuity relation,

$$V_{p1} A_{p1} + Q = V_{p2} A_{p2} \qquad \text{(A-25)}$$

Sketch (b) shows the flow condition when both sides of the dropshaft act as closed conduits. The inflow Q is again given, and therefore four unknowns, V_{p1}, V_{p2}, V_{p3}, and H_p, must be determined. Two characteristic equations plus two boundary conditions are needed. The continuity relation at the junction gives:

$$V_{p1} A_1 + V_{p3} A_3 = V_{p2} A_2 \qquad \text{(A-26)}$$

In this case the dropshaft acts as a surge tank described by a storage equation:

$$Q(t) - V_3 A_3 = \frac{dH}{dt} \qquad \text{(A-27)}$$

5. Diversion Structure

A typical diversion structure is shown in Fig. A-6. There is a dam of fixed height y_o located downstream from the intercepter. This dam diverts the dry weather flow into the intercepter. When there is storm water flow exceeding the amount diverted, there will

Appendix (Cont.)

be a flow over the dam. The diversion structure is represented by three stations for modeling purposes. There are six unknowns, V_{p1}, y_{p1}, V_{p2}, V_{p3}, and y_{p3}. The amount of flow diverted, Q_4, is assumed to be given. In addition to the two characteristic equations, four boundary conditions are required. Neglecting the storage effect, two continuity equations can be written.

$$V_{p1} A_{p1} + Q_4 = V_{p2} A_{p2} \tag{A-28}$$

$$V_{p2} A_{p2} = V_{p3} A_{p3} \tag{A-29}$$

The energy loss between station 1 and station 2 is neglected. Thus,

$$\frac{V_{p1}^2}{2g} + y_{p1} = \frac{V_{p2}^2}{2g} + y_o + y_{p2} \tag{A-30}$$

Finally, an equation describing the flow over the dam is needed. The flow over the dam may be that of a broad crested weir or an orifice depending on whether there is an open channel flow or a closed conduit flow. Within each of the two catagories there are also a number of different cases. For example, if y_3 is small, the flow over the dam is critical and the flow equation takes the form

$$Q_2 = C_D B_2 (y_1 - y_o)^{3/2} \tag{A-31}$$

in which C_D = discharge coefficient and B_2 = dam width. Another case is when y_3 is only slightly less than y_1. Then the flow equation changes to

$$Q_2 = C_D A_2 (y_1 - y_3)^{\frac{1}{2}} \tag{A-32}$$

The possibility of reverse flows was also included in the model

Appendix (Cont.)

6. Downstream End

There are sluice gates and a flood control pumping station located at the downstream end. The configuration is shown in Fig. A-7. The river stage y_2 is given. The sluice gate is closed if the water level in the sump is lower than the river stage. If the reverse is true, the gate may be instructed to open at a specified speed. Thus, the gate opening b is considered as known. If the water level in the sump exceeds the flood level, the flood control pumps will be turned on. Pumps and gates are also programmed to shut down or close when the water level in the sump falls below certain specified values.

A linear pumping rule given by

$$Q_p = (Q_p)_{max} \frac{y_1 - (y_1)_{min}}{(y_1)_{max} - (y_1)_{min}} \tag{A-33}$$

has been extensively used in this model. The equation for the outflow can take different forms depending on the relative values of y_1, y_2, and b. The sump storage equation is

$$V_1 A_1 - Q_p - Q_g = A_s \frac{dy_1}{dt} \tag{A-34}$$

in which Q_g is the outflow through the gate and A_s is surface area of the sump. A positive characteristic equation is also added to the list of equations used to solve for the downstream boundary conditions.

7. Relief Structures

The relief structures referred to herein are structures designed to divert part of a large storm runoff from one sewer system to another sewer system. Typically, a relief structure consists of flow constricting orifices and a diversion weir. It is designed to limit the flow downstream of the structure to a certain maximum value. Thus, the boundary condition at a relief structure is

$$0 \leq Q \leq Q_{max} \tag{A-35}$$

LIST OF ILLUSTRATIONS

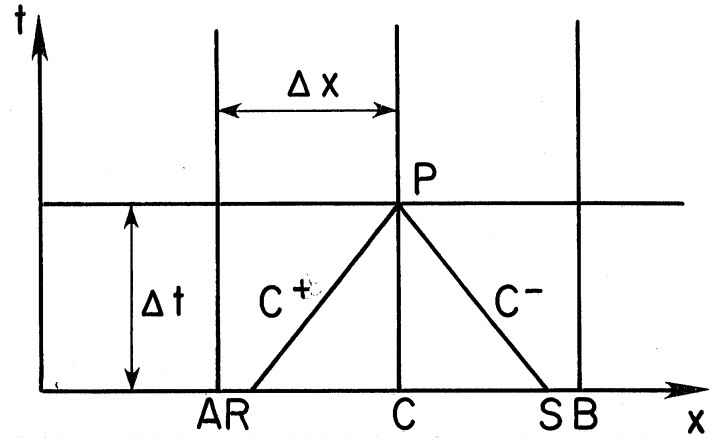

Fig. A-1 - Fixed Grid System for Single Phase Flow.

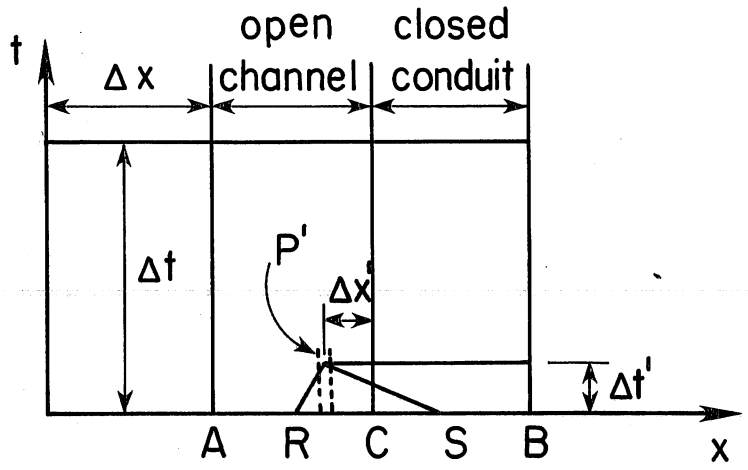

Fig. A-2 - Fixed Grid System for Mixed - Flow, Moving Interface.

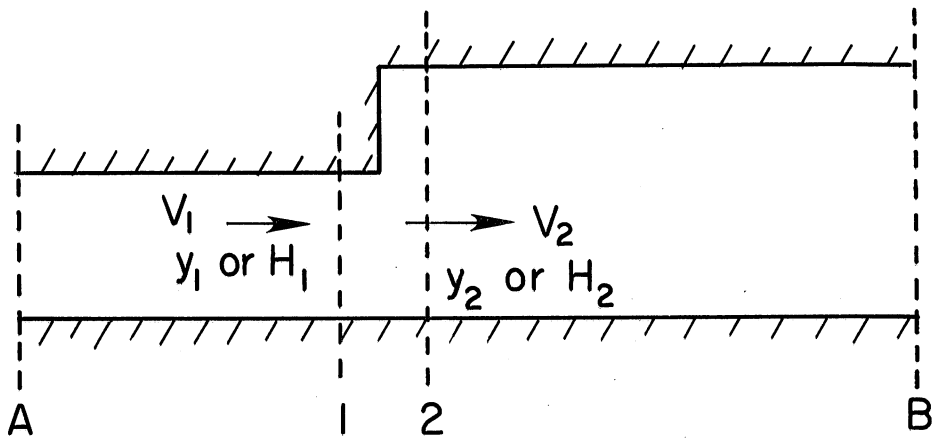

Fig. A-3 - Expansion Joint.

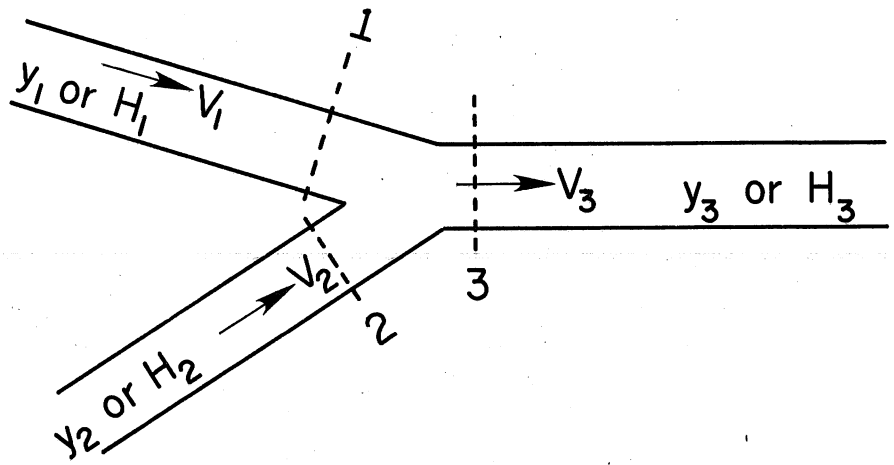

Fig. A-4 - 3-Way Junction.

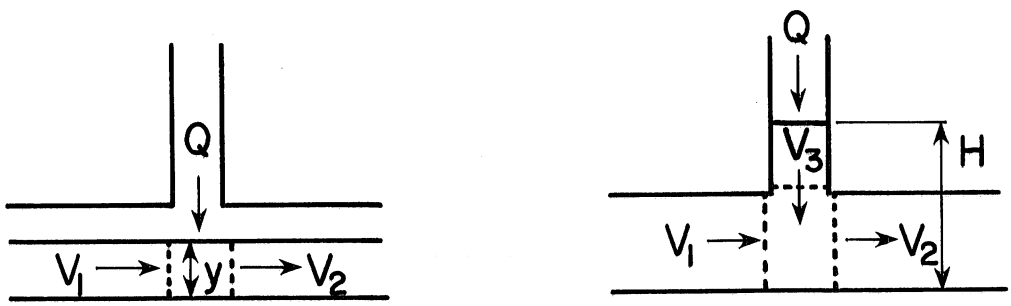

Fig. A-5 - Flow Conditions at Dropshaft.

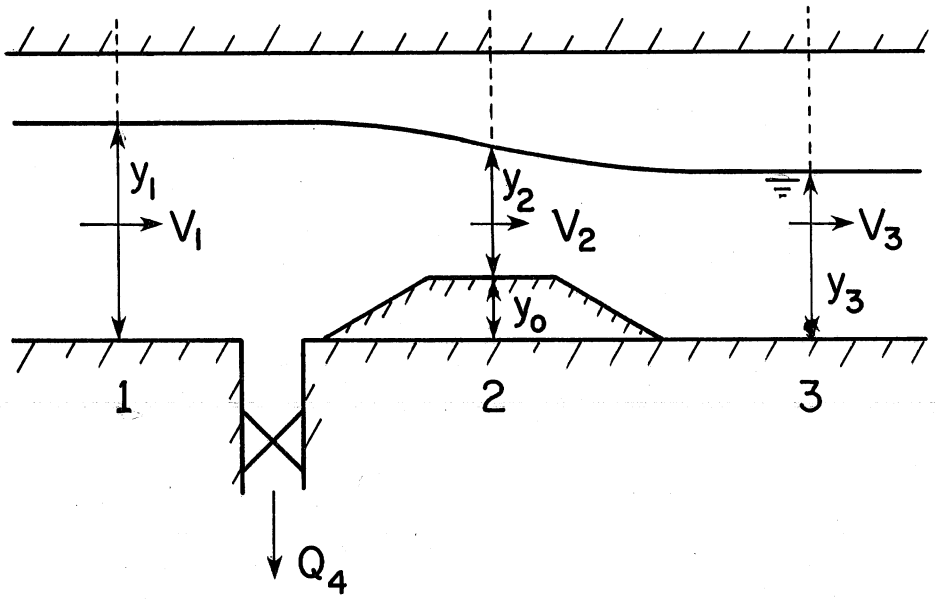

Fig. A-6 - Skematics of a Typical Diversion Structure.

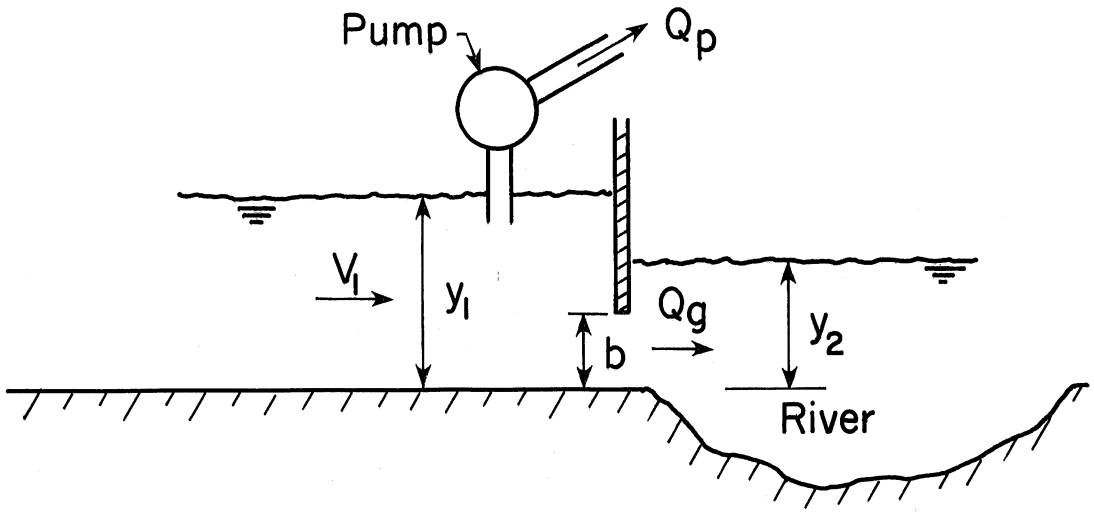

Fig. A-7 - Flow Condition at Downstream End.